Chapter 5

A REVIEW OF RELEVANT FILTERING TECHNIQUES

5.1 Introduction

In chapter 3 we defined the spectral characteristics of both our 'signal' and 'noise' waveforms. It was shown that the noise spectrum overlapped with the signal spectrum with the energy of the noise spectrum which overlapped the signal waveband being far less dependant upon sensor elevation than was the high frequency component. The objective of this review was to look at the filter options that were available which may have been relevant to the extraction of our magnetic signal from our measured waveform. We can define our filter requirements as follows.

(I) Zero or minimal modification of the signal.
(II) High noise rejection.
(III) Robust. Require minimal operator interference.
(IV) Be economic on computor CPU time.

Inevitably there were some compromises to be made between the above priorities.

Before examining particular filter operators in terms of the above priorities some filter design philosophies have been considered.

5.2 Filter design philosophies

White noise is mathematically defined (Sheriff, 1980) as

containing all frequencies with equal amplitude and random phase. The unwanted magnetic signals which we consider noise differ from white noise by consisting of only a specific frequency band. In favourable circumstances the unwanted signal is small in amplitude compared with the target signal and can therefore be separated by eye. In other circumstances where the noise is large in amplitude but occupies a different spectral band to the signal, it can be separated by filtering. In a third situation where the signal and the noise occupy the same spectral band and have comparable amplitude, then generally the signal and noise cannot be separated unless the precise shape of the signal is known. The situation encountered in this study, on first appearances was the latter.

Theory of signal extraction, interpolation and smoothing was written by Wiener (1949) to provide a method for designing the required filters. Another book, translated from Russian, was written by Wainstein and Zubakov (1962). They describe a method for the extraction of signals from random noise. Holloway (1958) combined all the smoothing and filtering information which was scattered widely in mathematical, statistical and scientific literature to explain smoothing and filtering processes. A review of filtering processes described during the period 1964-1971 was done by Grant (1972). Grant showed that filter design using Strakhov's method (Strakhov, 1964; Strakhov and Lapina, 1967) to modify the power spectrum applied only to the random noise. The spectral technique applied by Spector and Grant (1970) to distinguish between the spectra of signal and noise was appropriate to either random or non-random noise. Papers by Hahn (1965) and Lehman (1970) described the use of harmonic analysis to separate the potential fields of magnetic sources from different depths.

Figure 5.1 is a schematic diagram of the mathematical filters which were considered for application to the field data of this study. The 'Spike Rejection Filter' was a non linear filter developed for this data.

Linear filters were defined by Dean (1958) to have the following three properties. The first is superposition: the output of the

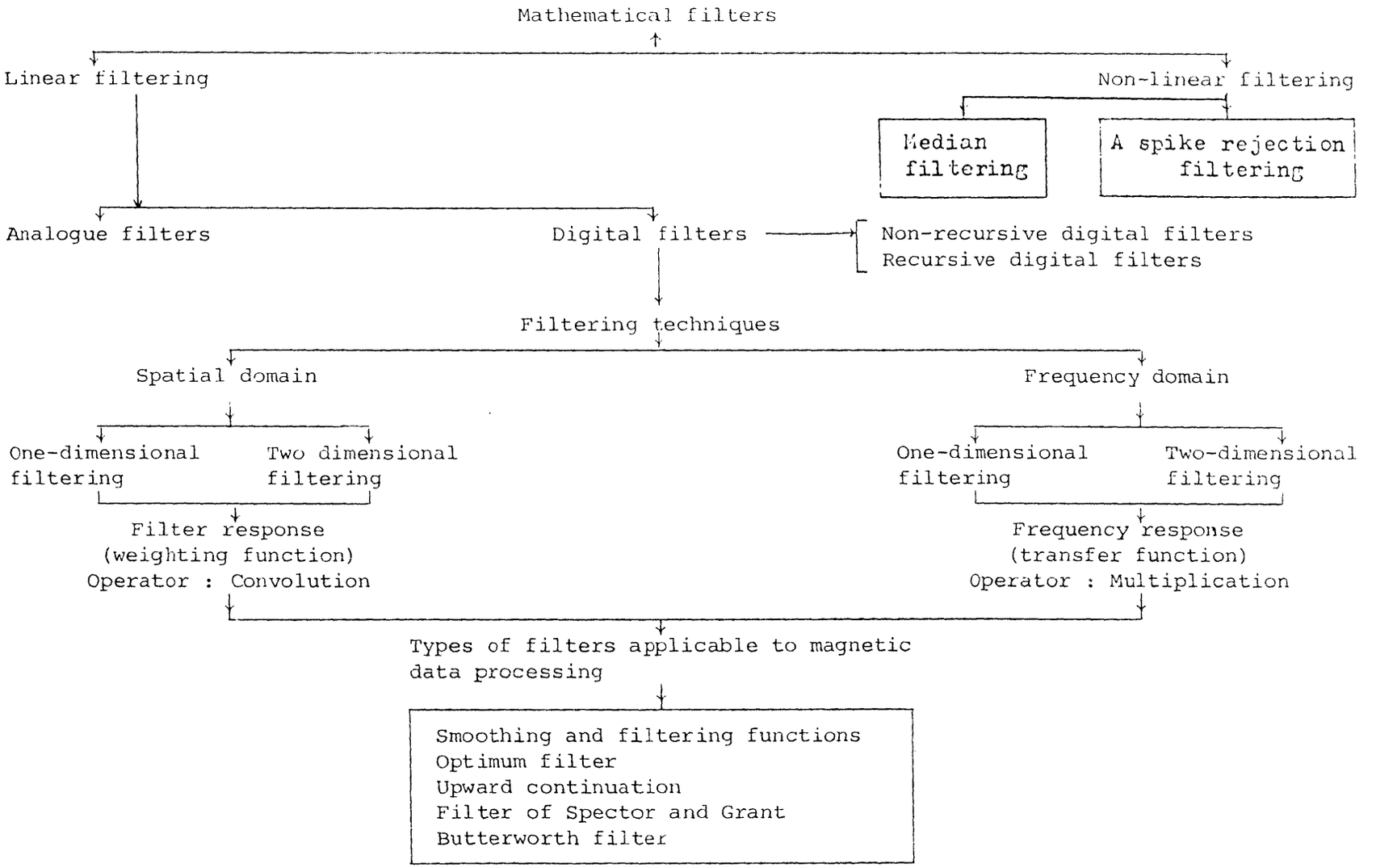

FIGURE 5.1: *Schematic diagram of the mathematical filters discussed and considered for application to the field data of this study.*

filter to a sum of inputs is equal to the sum of the outputs of the filter with each input applied separately. That is, if for each input $f_i(t)$ the output of the filter is $F_i(t)$, for the input $\Sigma_i a_i f_i(t)$ the output will be the sum $\Sigma_i a_i F_i(t)$. The second property states that the filter behaviour is independent of time origin. That is, if $F(t)$ is the response of the filter to an input $f(t)$, then $F(t-t_o)$ will be the response of the filter to the input $f(t-t_o)$. The third property states that the output of a filter depends only on the present and past values of the input, which means that a filter does not respond to an input before that input is applied.

Linear filtering (see Figure 5.1) can be subdivided into two groups. They are analogue filters and digital filters. Most of the mathematical filters are digital filters. There are two types of digital filter : recursive filters and non-recursive filters. Filtering techniques were mainly done in two-dimensional filtering or a map form in both spatial domain (Henderson and Zietz, 1949; Peters, 1949; Naidu, 1967; Clarke, 1969, Bhattacharyya, 1972), and frequency domain (Dean, 1958; Darby and Davis, 1967; Zurflueh, 1967). Transform operators are carried out by convolution with filter response or weighting function in the spatial domain or by multiplication with frequency domain or transfer function in the frequency domain.

Shanks (1967) designed a one-dimensional filter based on the concept of recursion. Recursive algorithm involves with a portion of already-calculated output which is continuously or discretely fed back to the input for computing the present output. Shanks (1969) and Shanks, Trietel and Justice (1972) considered the stability of the filter and synthesis of two dimensional recursive filters from a theoretical point of view. Bhattacharyya (1976) continued designing zero-phase two-dimensional recursive filters with a specified response in the frequency domain for processing potential field data.

Non-linear filter process does not obey the principle of superposition, nor do they have the property of frequency preservation as do the linear process : non-linear system may not be completely characterized by impulse or frequency response functions, nor may their output

signals be derived by transform methods or by convolution. The process may set a boundary for upper and lower limits of data series to be filtered. It is a process that is very similar to what an analysis would do by eye (Grant, 1972)

5.3 Smoothing and filtering functions

The smoothing operation was defined by Holloway (1958) as a convolution with a smoothing function or a filtering function. The smoothing function or the filtering function was a series of values called weights. The weights determine in what proportion each data point contributes to the estimate of the smoothed data value.

In designing the weights of the smoothing and filtering functions, designing techniques can be found in various standard textbook, e.g., Anders, Johnson, Lasaine, Spikes and Taylo (1964); Jenkins and Watts (1968); Otnes and Enochson (1972); Oppenheim (1975); Ota Kulhanex (1976) and Hamming (1977).

The first attempts to filter signal from background noise in the Cobar region were performed by hand to obtain a smooth curve (Skrzeczynski and Meated, 1977). Wilkes (1979) used Holloway's (1958) smoothing operation on running averages using odd numbers of observations with equal weights for a first approach to filterings. Then, Blackburn (1980) applied trend surface analysis to filter magnetic data. Later Gidley and Stuart (1980) applied the filter of Spector and Grant to remove near-surface signals from their carborne magnetic data at Elura.

The principal shortcoming of such filtering techniques was the fact that the operator was depending upon his subjective expectation of what the 'signal' component of the waveform should look like. The operator had no idea what component of the noise spectrum was being retained in his smooth profile. This study specifically aims at quantifying this parameter for each filter process in order that a true signal to noise ratio can be defined.

5.4 The Butterworth Filter

The Butterworth filter was recognized as being an important tool in designing a filter strategy for the data studied. It can not of course distinguish between signal and noise where they share the same spectral band.

The Butterworth filter has the properties of providing a very sharp cut-off and a flat response in the pass range. The cut-off frequency is readily defined and zero phase shift can be achieved. The response of an input waveform to Butterworth filtering is precisely predictable. These properties made the Butterworth filter the appropriate choice when low pass or band pass filtering was required. The zero phase Butterworth filter described by Blair and Spathis (1980) was adopted for this study. The filter is defined by the following squared magnitude function (Lynn, 1980):

$$\left|H(jw)\right|^2 = \frac{1}{\left[1 + (w/w_c)^{2n}\right]} \qquad (1)$$

where n is a positive integer and is called the order of the filter, w_c is the cut-off frequency of the filter.

Typical filter magnitude characteristics for n = 3,5 and 8 are shown in Figure 5.2. It is obvious that the 8^{th} order filter is quite a good representation of the amplitude response of an ideal low pass filter. But the phase response deteriorates (i.e. deviates from the ideal linear phase) as the n increases. Blair and Spathis (1980) gave a plot of phase response for n = 2 and 3 for a comparison. The plot is in Figure 5.3. This plot shows $\phi(w)$ as a function of w/w_c for both the second and third order Butterworth filters and clearly shows that the second order filter has a more linear trend over the pass band than does the third order filter.

However, Blair and Spathis (1980) have suggested that the third order Butterworth filter is probably a reasonable compromise between both amplitude and phase characteristics desirable for a low pass filter.

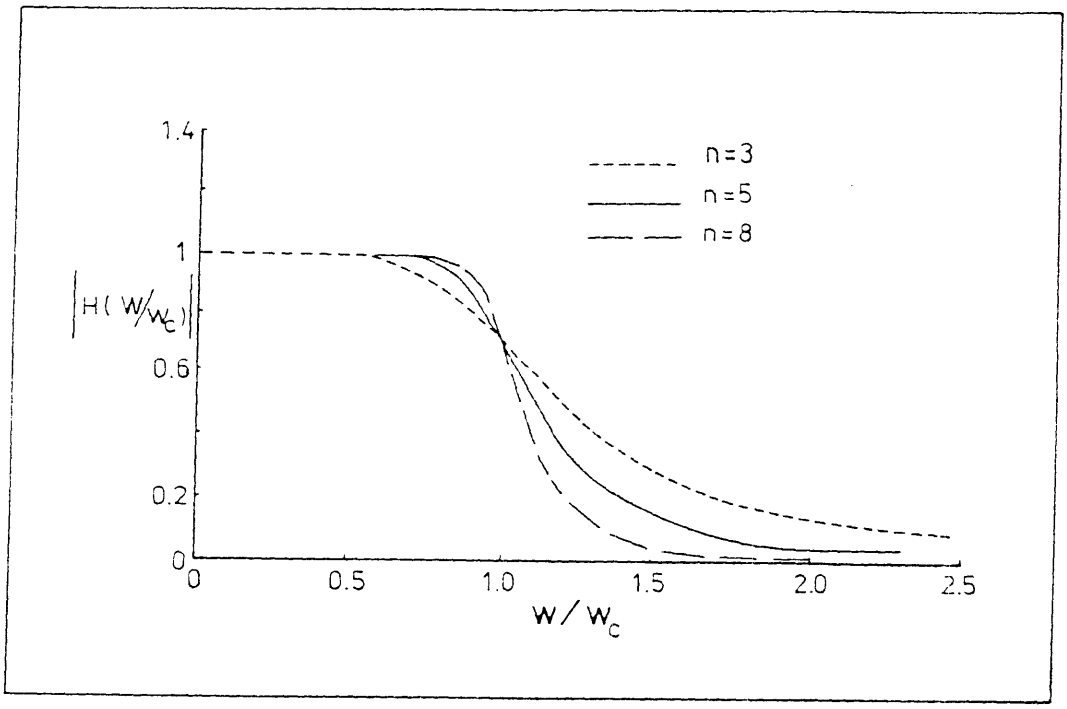

FIGURE 5.2: *Amplitude response of Butterworth analogue filter for n = 3, 5 and 8 (after Blair and Spathis, 1980)*

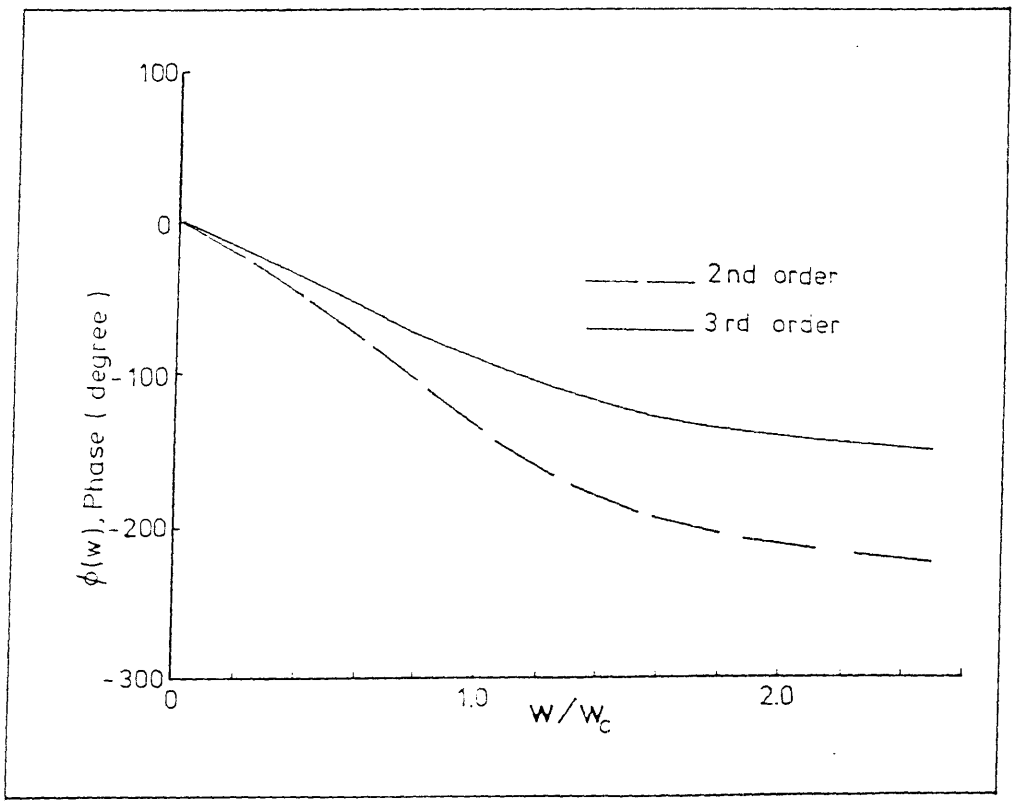

FIGURE 5.3: *Phase response of Butterworth analogue filter (after Blair and Spathis, 1980).*

For high order recursion filters, Blair and Spathis (1980) designed a low pass filter based on the application of the bilinear transform method to determine the recursive filter coefficients for the sixth order Butterworth filter. The filter has a z-transform given by:

$$H(z^{-1}) = H(c_1, z^{-1})\ H(c_2, z^{-1})\ H(c_3, z^{-1}) \qquad (2)$$

where c_n are constants, $c_1 = 0.5176$, $c_2 = 1.4142$, $c_3 = 1.9318$. So the filter can be synthesized by the application of the three recursions defined by equation (2).

Using the bilinear transformation given by the following equation:

$$S = \frac{2}{\Delta x}\left[\frac{1 - z^{-1}}{1 + z^{-1}}\right] \qquad (3)$$

where Δx is the sample interval between the data points, the quadratic factor for the sixth order Butterworth filter has the z-transform:

$$H(z^{-1}) = \frac{T^2 + 2T^2 z^{-1} + T^2 z^{-2}}{(T^2 + 2Tc + 4) + (2T^2 - 8)z^{-1} + (T^2 - 2Tc + 4)z^{-2}} \cdot \qquad (4)$$

where $T = 2w_c \Delta x$.

Recast the equation (4) in the form:

$$H(z^{-1}) = \frac{\dfrac{T^2}{(T^2 + 2Tc + 4)} + \dfrac{2T^2 z^{-1}}{(T^2 + 2Tc + 4)} + \dfrac{T^2 z^{-2}}{(T^2 + 2Tc + 4)}}{1 + \dfrac{(2T^2 - 8)z^{-1}}{(T^2 + 2cT + 4)} + \dfrac{(T^2 - 2cT + 4)z^{-2}}{(T^2 + 2cT + 4)}} \cdot \qquad (5)$$

This enables the series of recursions to be given by:

$$f_n = a_{10}x_n + a_{11}x_{n-1} + a_{12}x_{n-2} - b_{11}f_{n-1} - b_{12}f_{n-2}$$

$$g_n = a_{20}f_n + a_{21}f_{n-1} + a_{22}f_{n-2} - b_{21}g_{n-1} - b_{22}g_{n-2}$$

$$y_n = a_{30}g_n + a_{31}g_{n-1} - a_{32}g_{n-2} - b_{31}y_{n-1} - b_{32}y_{n-2}$$

where $a_{i0} = T^2/(T^2 + 2c_iT + 4)$;

$a_{i1} = 2a_{i0}$;

$a_{i2} = a_{i0}$;

$b_{i1} = (2T^2 - 8)/(T^2 + 2c_iT + 4)$;

$b_{i2} = (T^2 - 2c_iT + 4)/(T^2 + 2c_iT + 4)$; and

where x_i are the data values and y_i the filtered output.

This sixth order Butterworth filter has been written in FORTRAN IV for the DECSYSTEM-20 of the University of New England. The calculation part of the computer program is copied from Blair and Spathis (1980). This filter program is a zero phase recursion filter. To obtain a zero phase recursion filter, the computer program performs the following. The input data is filtered in the normal manner to produce a first output. This output is then reversed in direction and filtered with the same recursion filter to produce the final output signal.

In order to overcome the end effect problems encountered when a data set was truncated at either end of the survey line, a base field value was first subtracted from the data. Next, an exponential taper of length one eighth of the data profile was added to each end of the data to bring it to the nominated base field value. The importance of this process of 'detrending' and 'end tapering' the data is displayed in Figure 5.4.

The end effects of the Butterworth filter were effectively eliminated by this procedure.

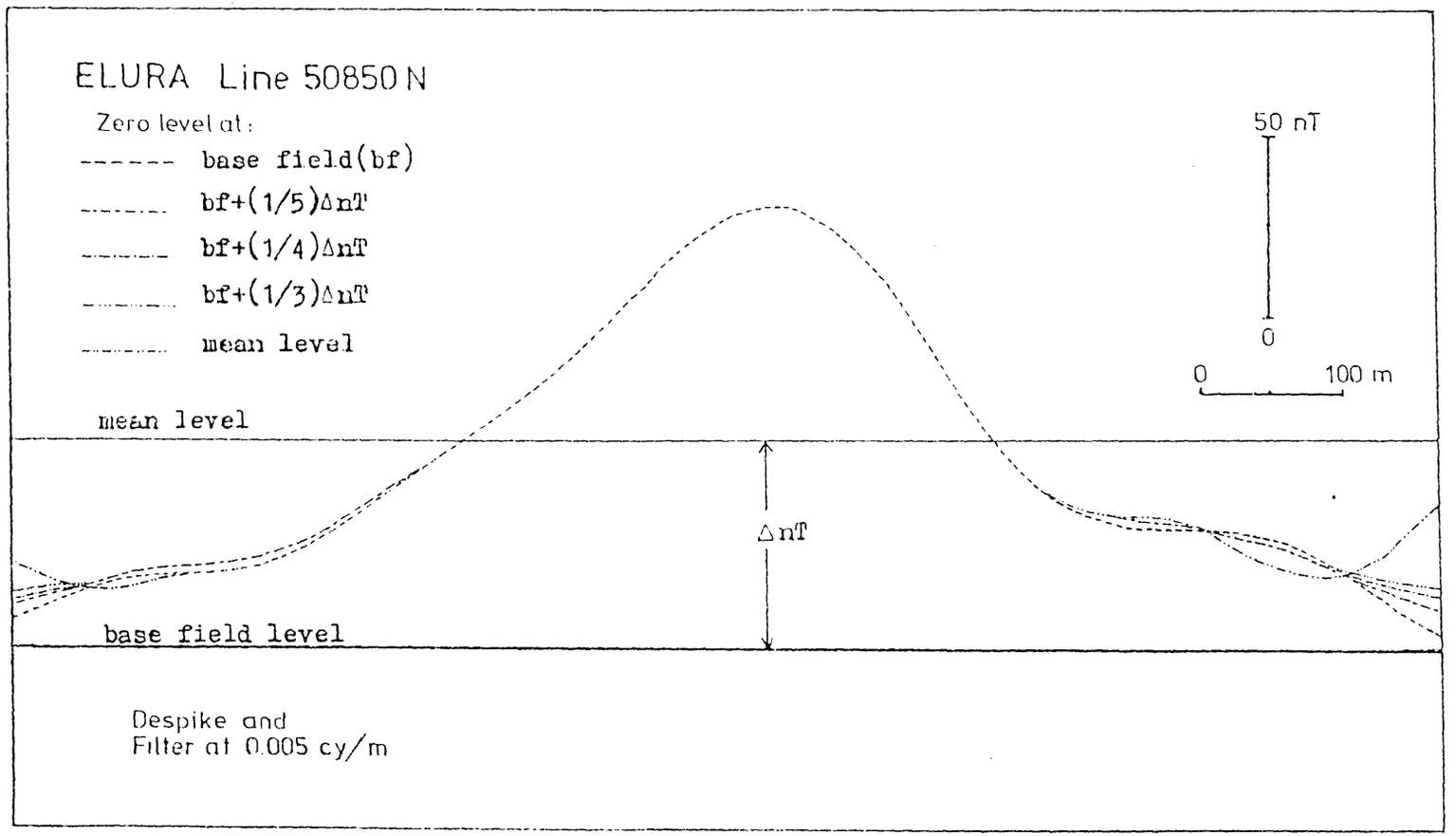

FIGURE 5.4: *End-effects when zero level is not properly chosen. Both ends of the filtered curve are dragged up when zero level is at mean level. The problem was overcome by first estimating a base field level and then adding an exponential truncating function of length one eighth of the data profile to the ends of the profile.*

The computer program which was used to perform Butterworth filtering was listed in Appendix III.

5.5 Upward Continuation

The upward continuation filter synthesizes the magnetic profile that would be recorded at one sensor elevation from data recorded at another elevation.

The Filter operator for upward continuation was computed from the equation (Peter, 1949; Henderson and Zietz, 1949; Henderson, 1960):

$$\Delta T(x,y,z) = \int_{-\infty}^{\infty}\int_{-\infty}^{\infty} \frac{(z/2\pi)\cdot \Delta T(\alpha,\beta,0)}{\left[(x-\alpha)^2 + (y-\beta)^2 + z^2\right]^{3/2}} \, d\alpha \cdot d\beta \qquad (1)$$

where $z < 0$, $\Delta T(\alpha,\beta,0)$, and $\Delta T(x,y,z)$ are the magnetic field either vertical or total field component (Grant and West, 1965; Henderson, 1970; Robinson, 1970) at the level 0 and z respectively. This equation satisfies the Laplace equation $\nabla^2 A = 0$, where A is magnetic potential anomaly.

In one-dimensional form, equation (1) becomes (Dean, 1958; Tsay, 1978):

$$T(x,z) = \int_{-\infty}^{\infty} \frac{z/\pi}{z^2 + \alpha^2} \cdot \Delta T(x-\alpha,0)\, d\alpha \qquad (2)$$

$$= \int_{-\infty}^{\infty} F(x,z) \cdot \Delta T(x-\alpha,0)\, d\alpha \qquad (3)$$

where

$$F(x,z) = \frac{z/\pi}{z^2 + x^2} \qquad (4)$$

$F(x,z)$ behaves like filter operator or weighting function of upward continuation, and convolutes with magnetic field at $z = 0$. That is,

$F(x,z)$ is acting as a filter response with input $\Delta T(x)$ and gives the output $\Delta T(x,z)$. This filter is an ideal filter because:

$$\int_{-\infty}^{\infty} \frac{z/\pi}{x^2 + z^2}\, dx = \frac{1}{\pi}\left[\tan^{-1}\left(\frac{x}{z}\right)\right]_{-\infty}^{\infty}$$

$$= 1 , \qquad \text{for all } z .$$

If transforms $F(x,z)$ to frequency domain, the frequency response of the upward continuation process will be:

$$Y(s) = \int_{-\infty}^{\infty} F(x,z)e^{-isx}\, dx$$

$$= \int_{-\infty}^{\infty} \frac{z/\pi}{z^2 + x^2}\, e^{-isx}\, dx$$

$$= e^{-z|s|} \qquad (5)$$

where s is angular frequency in cycles per unit length and $i = \sqrt{-1}$.

Figure 5.5 shows the filter response of equation (4) and the frequency response of equation (5) when z is very large and very small (Tsay, 1978). If z is very large ($z < a$), rate of decrease is very slow as $|x|$ increases. $F(x,z)$ spreads out very wide along the x-axis and the filter is a narrow band pass filter in the frequency domain. If z is very small ($z > 0$), then $F(x,z)$ dies off very quickly as $|x|$ increases, so $F(x,z)$ has a very narrow form close to $x = 0$. This becomes a wide band pass filter in the frequency domain.

The important observation concerning the application of this filter to the present situation is that regardless of the size of z, the filter passes the low frequency component of the waveform and attenuates the high frequency. The Butterworth filter does the same thing but with a sharper and more readily controlled cutoff frequency. The same observation of the upward continuation filter response explains why the low

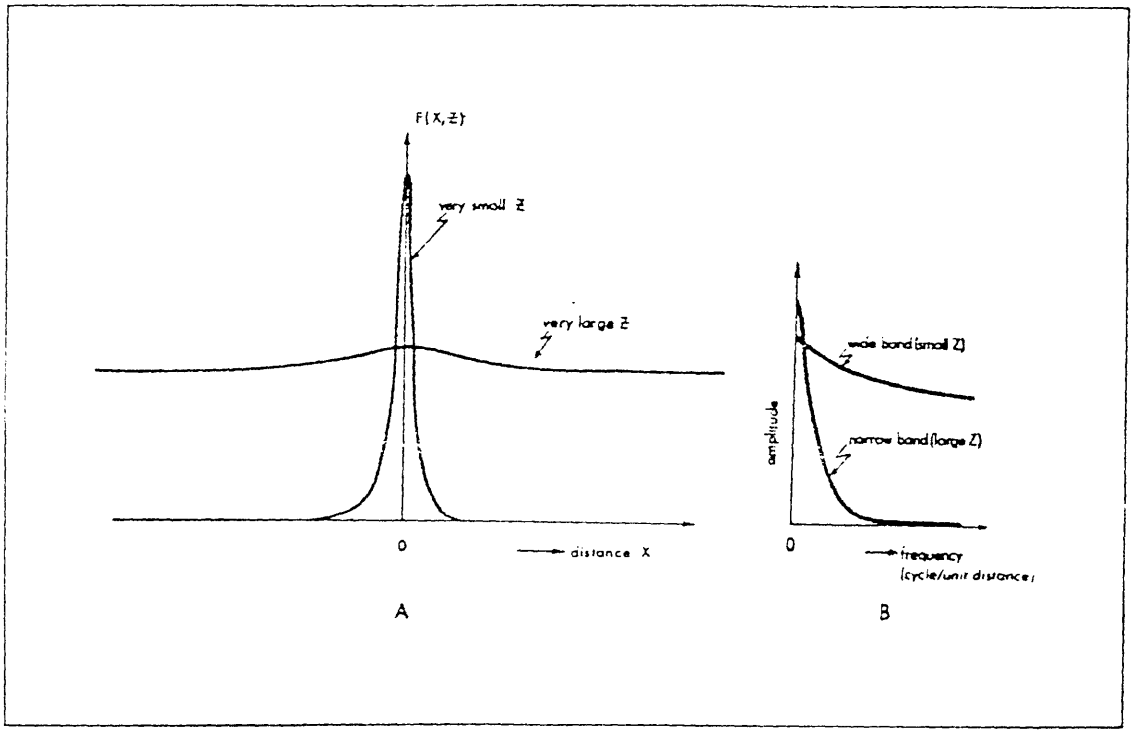

FIGURE 5.5: *Filter response F(x,z) at different levels (z) in spatial domain (A) and in frequency domain (B) (from Tsay, 1978).*

frequency component of the noise waveform was not severely attenuated when data was collected by airborne survey.

While upward continuation was a useful process for examining the behavior of magnetic profiles of different survey elevations, it was not considered a desirable alternative to the Butterworth filter when controllable low pass filtering was required.

5.6 The Filter of Spector and grant

This type of filter is based on the spectrum of magnetic bodies at different depths. An expression on the amplitude spectrum was first given by Bhattacharyya (1966). Then, Spector and Grant (1970) developed a technique based on Bhattacharyya's expression to identify two ensembles of sources from the energy spectrum of magnetic anomalies.

It should be noted that Spector and Grant had a specific objective in applying their technique. That was to enable the signal and the source to be 'identified' from the data spectrum and to enable a depth to the source to be calculated. Their technique is not a filter in the sense that signal and source can be completely separated. A signal to noise ratio can not be defined nor can the signal be isolated for later processing.

In spectral analysis, separation of signal and noise yields two incomplete partial fields as follows (Hahn, Kind and Misha, 1976):

a) If the spectrum, for example, see Figure 5.6 is cut at f_a and attributes the waves $f = 1 \ldots\ldots f_a$ to the lower layer and the rest to the upper layer. Some partial fields at frequency higher than f_a are missing which means a more or less strong smoothing and a loss of detail.

b) Some partial fields at frequency lower than f_a absent. This results in a loss of the large-scale features with only the smaller details remaining. This is not a desired filter. Gupta and Romani (1980) also comment

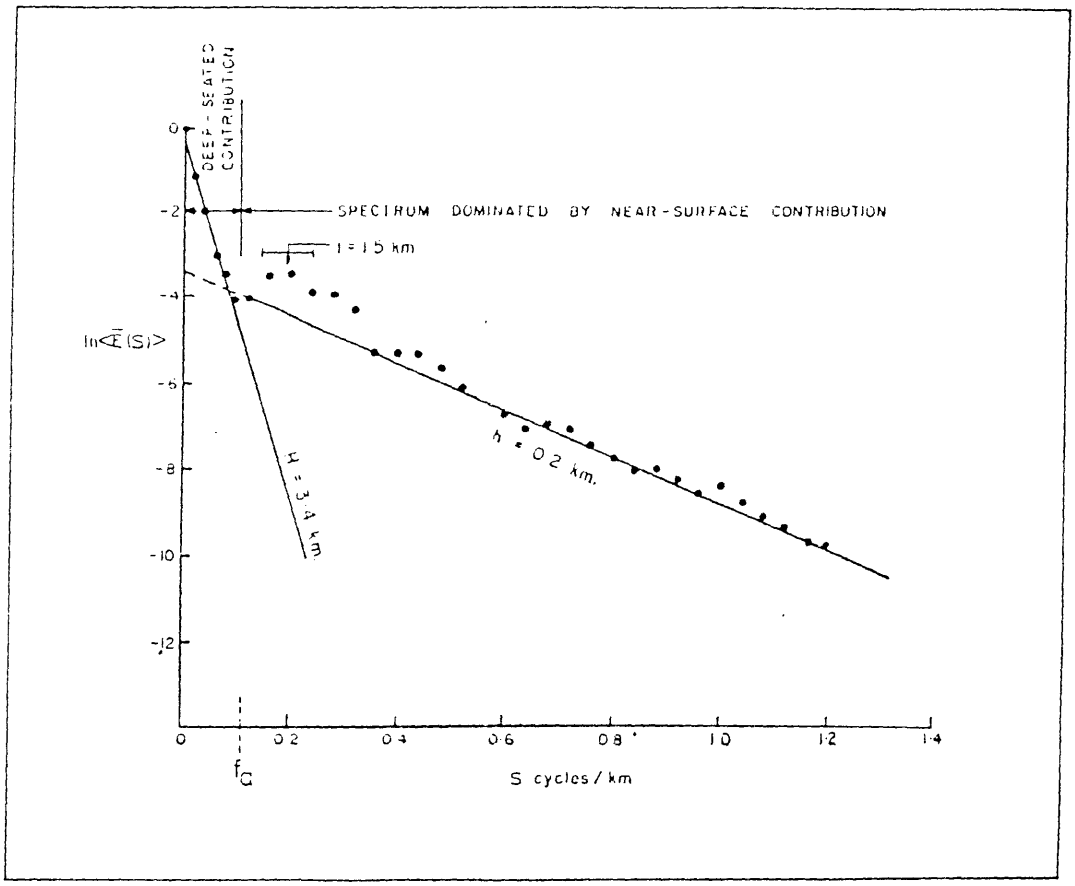

FIGURE 5.6: *Energy spectrum of the deep-seated body and the near-surface contribution from the Central American aeromagnetic map (taken from Spector and Grant, 1970).*

that the filter design by the spectral factorization technique is dictated by the clarity of the slope change between the short- and long-wavelength features.

Having identified the two linear segments of the plot (Figure 5.6) Spector and Grant (1970) showed that the slope of each segment gave the depth to the top of the component waveform source. The method was applied to the Elura data in Chapter 6 but was not further considered as a relevant filter.

5.7 The Median Filter

The median filter was succinctly discussed by Claerbout and Muir (1973) under the title 'Robust modelling with erratic data'. The advantage of the method appears not to have been greatly appreciated for automatic data conditioning, despite a fundamental paper by Gallagher and Muir (1981), who came to the conclusion that iterative median-value-window filtering could be used to separate a waveform into its signal and noise waveforms. The only paper recently on the subject is one by Bednar (1983).

In median filtering the effect of sliding a 3 point window over a data waveform is to replace the middle value by the median value of the three points. Any point that is a maximum or minimum value along the profile can never be a median value and consequently it must be replaced by one of its neighbours. The process is particularly effective in recognizing a data 'glitch' or a single data value which has been corrupted electronically or by manual error. The single glitch or spike has a broad band spectrum which may contain significant energy in the signal waveband.

The overlap of signal and noise spectra can not be removed by linear filtering. Detection and replacement of a glitch before linear filtering overcomes the problem.

The concept of a single glitch or spike may be extended to cover intense amplitude magnetic features of finite width. The user of the filter must make a subjective decision as to what is the maximum width of a spike like feature which he will define to be 'noise'. In exploration for deep, large targets such as those of economic interest as potential base metal targets, the maximum spike width may be defined as great as 25 metres. Inspection of the data from the Elura study (Appendix I) reveals that the extreme amplitude noise feature all have widths up to but less than 25 metres. A median filter which is required to replace up to N data points requires a window of 2N+1 data points. In the case of the Elura data which was sampled at 0.25 metre intervals, the rejection of extreme amplitude features of width up to 25 metres requires a window value of 201 data points. It must be emphasized at this point that the application of the median filter is not required to remove all the noise from the magnetic waveform. It is only required to remove the extreme amplitude noise features. Thus the user of the median filter is not required to make subjective decisions about the full characteristics of the noise but instead only a subjective judgement about what is considered an extreme value. In practice this decision can be easily made.

The great advantage of using the median filter to perform rejection of extreme amplitude, short wavelength features is that it is 'robust'. Having specified the required window, the process can be performed automatically without intervention by the user. The main disadvantage of the median filter is that for window values as large as 201 the demand on computer CPU time is considerable. As a guide, performing a 201 point median filter through a 4000 data point profile (i.e. 1 kilometre survey line at Elura) required 12.6 minutes of CPU time using a DECSYSTEM-20 main frame computer. The median filter also truncates either end of the magnetic profile by the distance equal to half the window length.

5.8 A Spike Rejection Filter

The problem of recognizing and replacing extreme amplitude localized magnetic noise features was addressed in the discussion of the median filter. While the median filter provided a solution to the problem it was excessively demanding upon computer CPU time. Consequently

an alternative criteria was sought for identifying spike-like noise features and for replacing them by magnetic data values which would not influence the low frequency spectrum of the magnetic profile. In the Spike Rejection Filter proposed below, the same arguements concerning the legitimacy of user defined noise spike characteristics apply as proposed under the section on the median filter.

Spikes may be recognized by eye due to their distinctive signature. They exceed the highest probable amplitude expected from a signal and they are very narrow in width. A coarse test for a spike could be to accept, as good data, only those measurements falling between a selected amplitude range significantly greater than any probable signal amplitude. In areas where the signal or regional gradient extend over a large range, the despiking range must also be large, in which case the technique is not very discriminating. Another test which is suitable for some despiking applications is the gradient test. By sequentially testing the difference between each new data point and the last accepted data point, rapid changes in gradient reveal a spike. In smooth data this test criterion is effective, but it does not work in the present situation because the high frequency component of the noise profile contains local gradients which exceed the slope of the larger spikes of cultural or maghemite origin.

The criterion adopted here for recognizing spikes was to compare each new data value along a profile with a smooth curve through the preceding data points.

To this end, a running average serves as an effective reference. If the new data value varies up or down from the last running average by more than a defined amount, then a spike is recognized. The length of the running average is called the 'WINDOW' and the acceptable limits by which the data point under test can exceed the reference is called the 'RANGE'. Clearly, the profile must be tested in both directions in order to eliminate the possibility of a spike evading the test because it occurred in the initial WINDOW of the first pass of the spike recognition process.

Having recognized a spike in a data profile, we need to make an automatic estimate of a good value to replace that being rejected. While great effort could be expended in predicting the best estimate of a replacement, it is found that in the present application this is not warranted. The most convenient replacement value to use is the value of the preceding running average. The accuracy of this estimate will vary with the running average WINDOW length and the local gradient of the signal waveform. However, only a first order estimate is necessary. The two requirements of the despiking procedure are to detect a spike and then attenuate it sufficiently to remove its low frequency component from the signal bandwidth. Figure 5.7 depicts the influences of despiking on the low frequency spectrum of a magnetic profile. Figure 5.8 demonstrates the effect of the WINDOW choice and the spike replacement value in the worst case situation of a broad spike anomaly occurring on the peak of a magnetic signal anomaly.

Note: In each of Figures 5.7 and 5.8, curve 1 is the spectrum before despiking. Curves 2, 3 and 4 are the spectra after despiking using WINDOWS of length 50, 100 and 500 data points respectively. These spectra demonstrate the importance of despiking in attenuating that component of the spike-like anomalies which has a wavelength in the signal band of 0 to 0.005 cycles/metre. Curves 2, 3 and 4 also verify that the choice of WINDOW in the spike replacement procedure is not critical within the guidelines proposed below.

The running average is a convenient smoothing function employed here to provide a stable reference for detecting the presence of a spike. It is also used to provide an estimate of a suitable replacement value when a spike has to be removed. The running average is a simple low pass filter where the cutoff depends upon the WINDOW length. In this application the WINDOW must be sufficiently long to filter most of the energy of the noise waveform and hence provide the smoothing necessary to provide a stable reference. The maximum gradient of the smoothed reference must be significantly less than the minimum gradient of a 'spike-like' anomaly. This criterion defines the minimum WINDOW length. If the two gradients are not sufficiently different then a criterion for

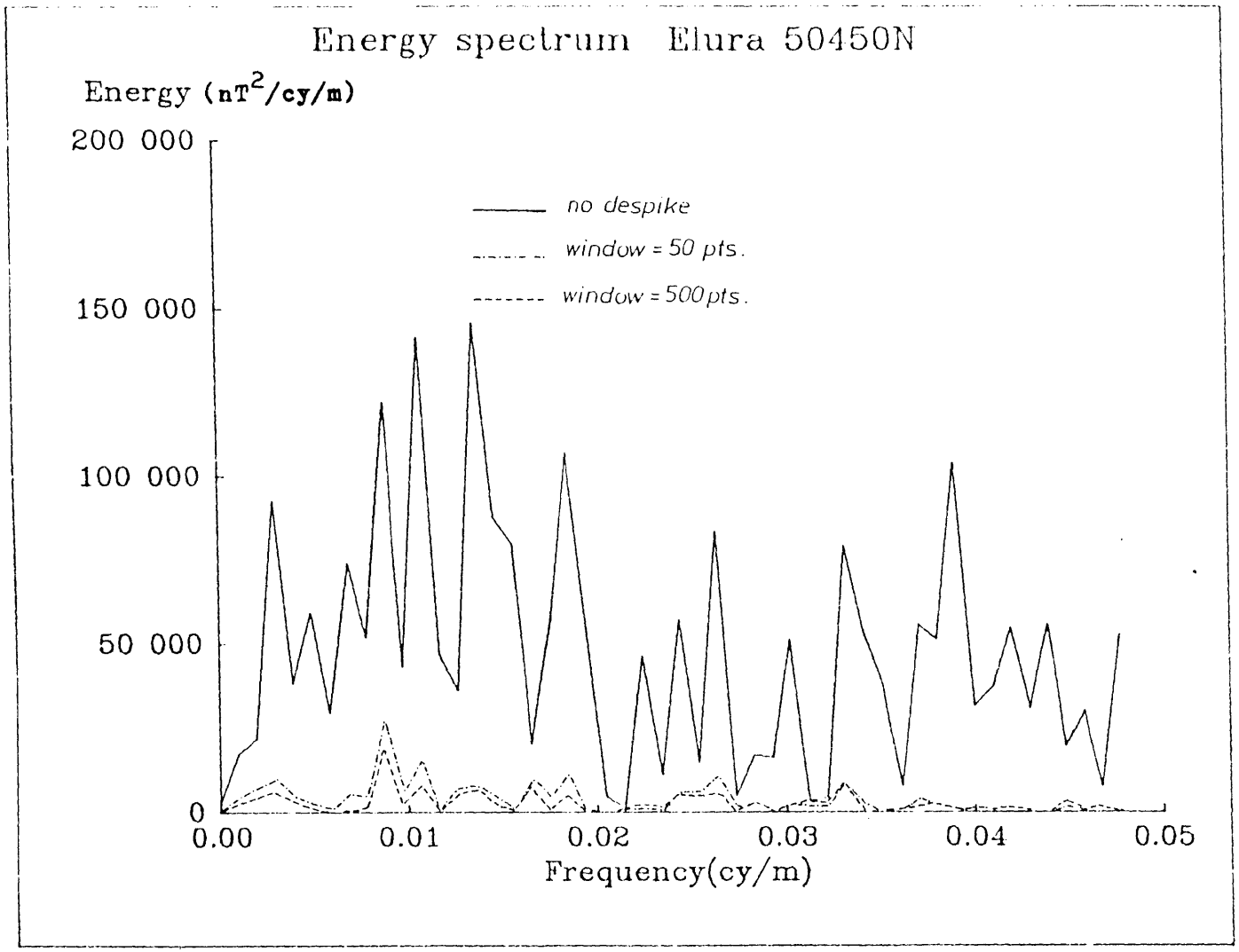

FIGURE 5.7: *Spectra computed for Elura line 50450N which was considered to contain noise only and no signal anomaly.*

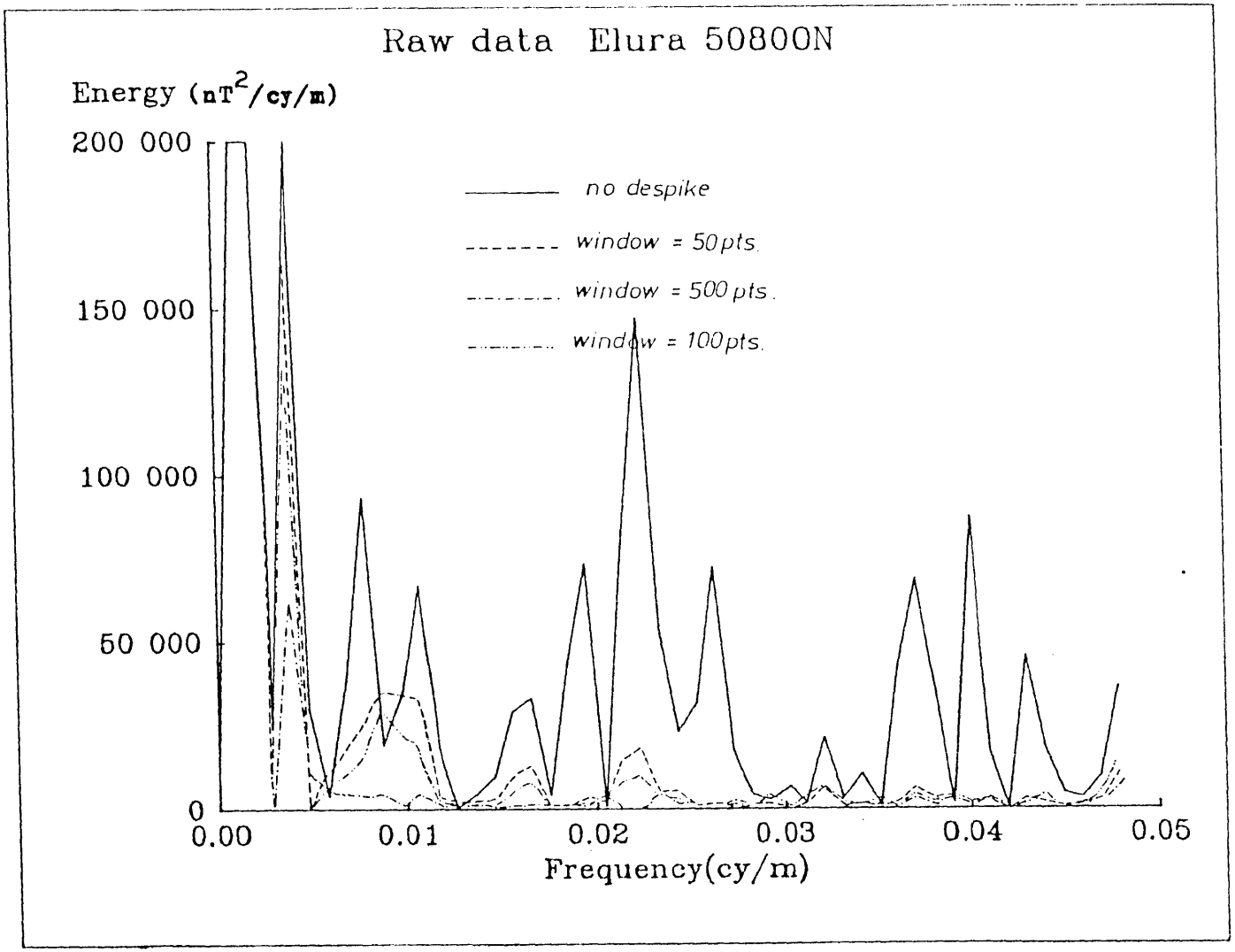

FIGURE 5.8: *Spectra computed for Elura line 50800N which contained both the Elura orebody anomaly and noise. Note that from the origin to 0.003 cycles/metre the four curves were identical.*

automatically discriminating between them becomes unreliable. Clearly, the minimum WINDOW length must depend upon the users definition of a 'spike' and upon the minimum widths of any anomaly which we would consider 'signal'. If we are seeking localized signal anomalies, then we must be more strict in our definition of a noise spike if we are to reliably distinguish between the two.

The maximum WINDOW length applicable depends upon two considerations. For the despiking process to work the WINDOW must be less than half the profile length. Spikes occurring within the initial WINDOW at the beginning of the profile will not be detected until the second pass of the process commencing at the other end of the profile. The second consideration is that the maximum gradient of the reference profile produced by the running average must be greater than the maximum gradient of the geological signal. Other-wise the signal will be interpreted as a spike as previously discussed.

The considerations presented for defining the WINDOW range may be generalized by the following rule of thumb:

> The WINDOW length must be chosen such that it falls between the half width of the broadest anomaly to be interpreted as a 'spike' and half width of the narrowest anomaly to be interpreted as 'signal' provided the WINDOW is less than half the profile length.

In most mineral exploration situations the above definition allows a great deal of freedom as the half width of any anomaly considered of significance will be many times greater than the half width of spike-like noise.

Figure 5.9 demonstrates the potential disaster of not obeying the above rule. In this example, a 10 data point WINDOW (2.5 metres) was adopted. While this was satisfactory for detecting the more 'ideal' spikes, it fouled on a 'broad' spike arising from a nearby piece of large machinery. The smooth reference function was able to track the flank of the spike for a considerble distance before recognizing it as a spike. By the time the spike was detected, the reference was outside the RANGE of the signal and the process failed.

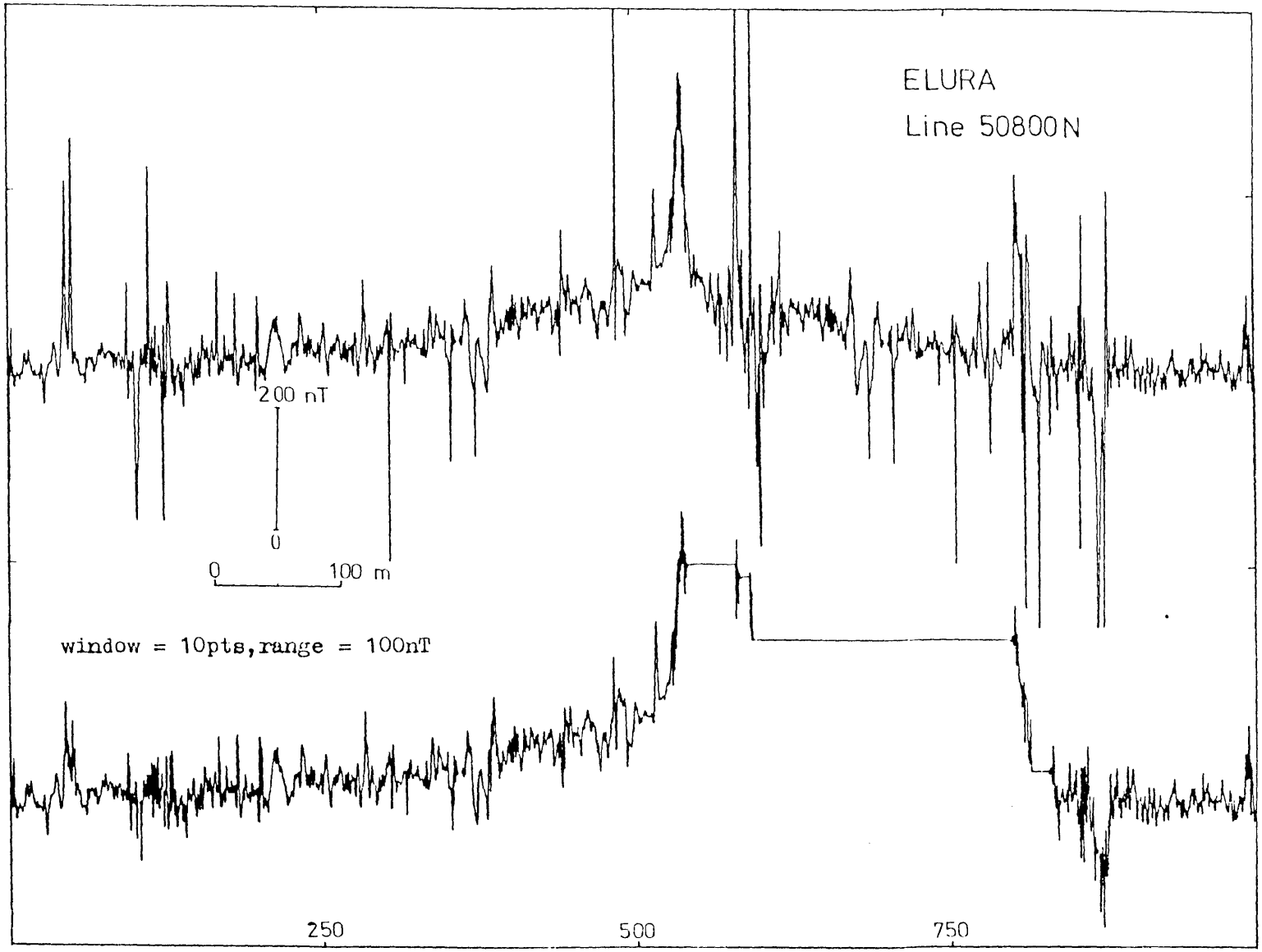

FIGURE 5.9: *Raw magnetic data recorded across line 50800N at Elura. And the corresponding line is after despiking using the recommended RANGE of 100 nT, but a WINDOW which was too short(2.5 metres). While the WINDOW was adequate for the 'ideal' very narrow 'spike-like' features it was too narrow for the 'broad spike' at 550 metres and the despiking process failed.*

In the case of the Elura study, the broadest magnetic disburbance due to interference from noise sources had a half width of about 25 metres (100 data points). The Elura mineralization anomaly, on the other hand, had a half width of 170 metres (680 data points). Using the rule proposed for determining the appropriate WINDOW, we find that the WINDOW should be between 100 and 680 data points. This range is very broad, confirming that there is little difficulty in determining a WINDOW which will effectively enable a spike to be detected(See Figure 5.10).

The choice of value for the RANGE by which a data point must exceed a profile reference before being classified as a 'spike' will depend upon the choice of profile reference. We have chosen a running average as our profile reference and hence the appropriate choice of RANGE will depend upon the running average WINDOW. However, the RANGE choice is only critical when the WINDOW is very short. In this case, the reference becomes erratic, requiring the RANGE to be very large if the process is to be reliable. A large RANGE implies that only the very high amplitude 'spikes' can be detected. However, if the WINDOW is chosen according to the proposed rule above, then the choice of RANGE is far less important because of the stability of the reference function. In this case, its value can closely approach the normal noise envelope of the data. The despiking procedure then becomes exceedingly effective. We propose that the following rule be adopted for selecting a RANGE value after the rule for selection of WINDOW has been followed.

The RANGE value shall be chosen to equal the value of the normal noise envelope.

Note: a) The RANGE is applied above and below the reference function.

b) The normal noise envelope is considered to be the peak to valley ~~value~~ of the noise envelope excluding spikes.

In recognizing and removing spikes before linear filtering, the low frequency noise source can be recognized and removed. Figure 5.11 shows the effect of despiking on the filtered profile of line 50800N at Elura. While inspection of this figure does not permit a

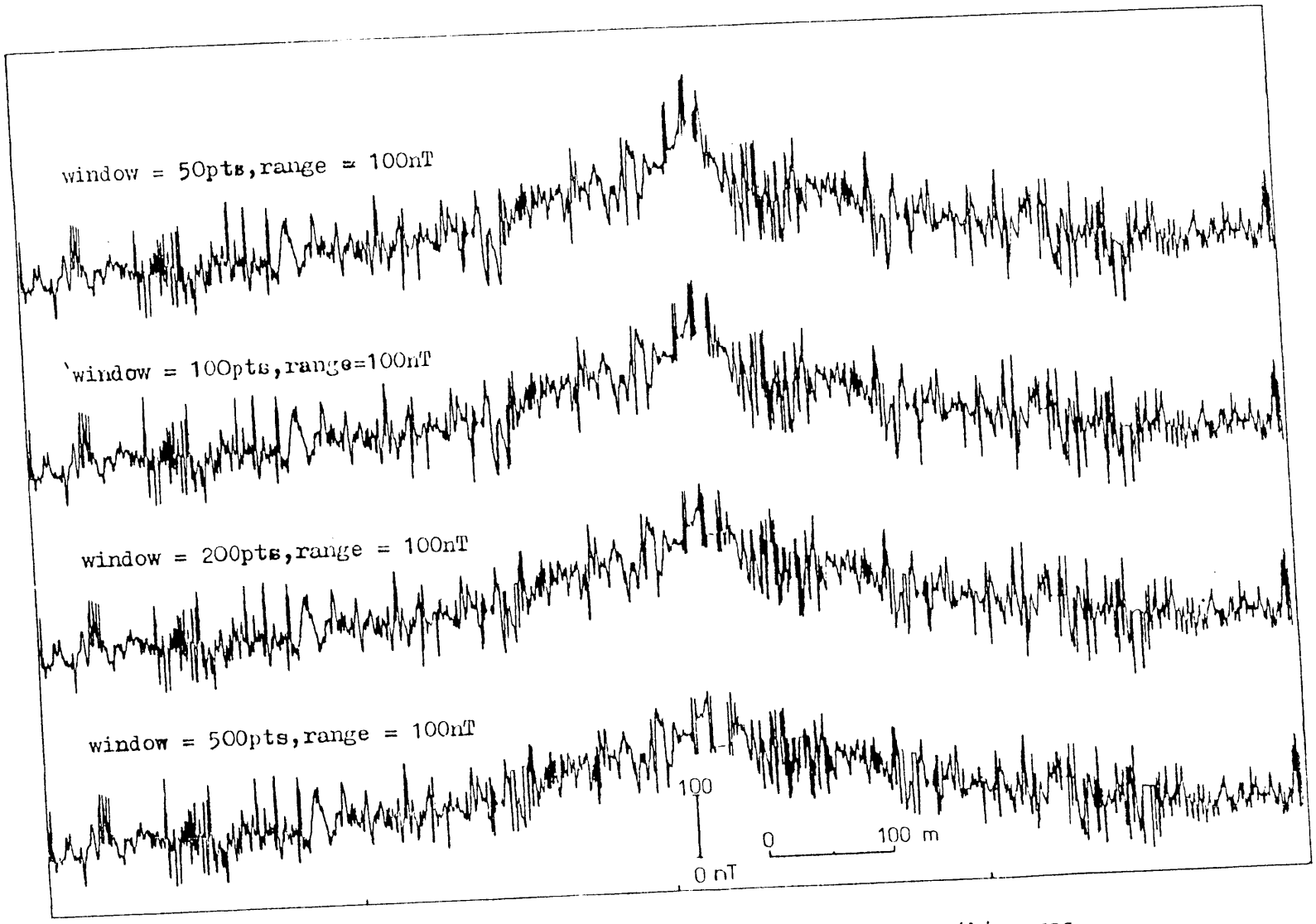

FIGURE 5.10: *The same magnetic data as Figure 5.9 but despiking was performed with WINDOWS set at 50, 100, 200 and 500 data points. Each of these WINDOW values detected all spikes, but each resulted in a different replacement value. Figure 5.8 demonstrated that these differences in replacement value were of little consequence to the low frequency spectrum of the profile.*

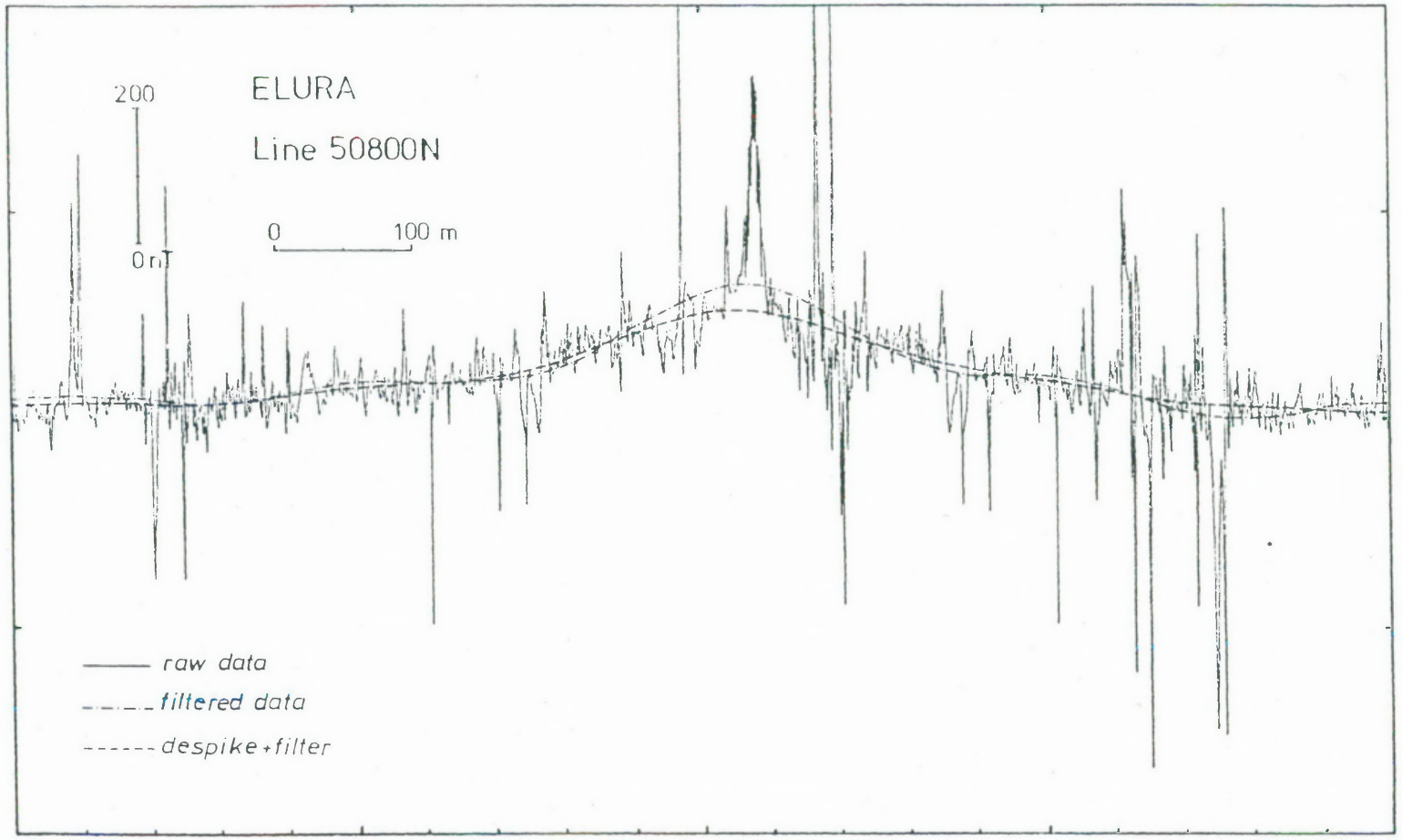

FIGURE 5.11: *Line 50800N from Elura showing the raw data and the low pass filter output computed before and after despiking. While inspection of this figure does not permit a judgement of which filtered profile correctly represents the anomaly due to the orebody, the difference can be clearly seen. The spectra of Figure 5.7 confirms that despiking preceding linear filtering produces the ~~varid~~ result.*

varied

judgement of which filtered profile correctly represents the anomaly due to the orebody, the difference can clearly be seen. The spectra of Figure 5.7 confirms that despiking preceding linear filtering produces the valid result.

The advantage of the spike rejection filter proposed here is that it achives the desired result with economy of computer CPU time. Comparing this parameter between the median filter and the proposed spike rejection filter we found that for the same data and the same width of spike to be rejected the median filter required 12.6 minutes of CPU time while the proposed filter required just 2.8 seconds.

The disadvantage of the proposed method however was that the process may become unstable if an inappropriate choice of WINDOW and RANGE is made.

A Fortran program for performing spike rejection as proposed here was provided in Appendix IV.

5.9 The Wiener Filter

The Wiener filter was mentioned here because in many situations where the signal and noise spectra overlap it is still possible to separate the two. The method was described by Robinson and Treitel (1967). The process assumed that the noise spectrum was 'white' and that the character of the signal was known. The process described by Robinson and Treitel(1967) required the input of the estimated desired signal and the input of noisy data waveform. The spectral energy existing in the difference between the actual filter output and the desired output was then minimized by least squares adjustment. The Wiener filter is also known as an 'optimum' or 'least squares' filter.

The Wiener filter was not considered to be appropriate in the present application because of the undesirability of prejudicing the output by subjectively estimating the desired signal characteristic. While it might be argued that is a case study such as Elura where the

desired output was in fact known, the Wiener filter could have been applied and a measure of its performance determined. However such a result would have little practical value. In applied exploration some constraints can be defined in describing the desired signal but the range of signal characteristics within those constraints still remained infinite.

5.10 Conclusion

The filters described in this chapter were quantitatively assessed in chapter six after their application to magnetic data from the Elura area. The Wiener filter was not applied to Elura data after it became apparent that because of the inherant approximations involved it could not compete with the very good results obtained by other methods.

Chapter 6

ASSESSMENT OF FILTER OPERATORS IN THEIR APPLICATION TO MAGNETIC DATA FROM ELURA

6.1 Introduction

In chapter five filter operators were discussed which for one reason or another were considered relevant to this study. Hand smoothing, running averages and trend surface analysis were discussed because these were the methods used by previous authors in their attempts to apply magnetic exploration methods to noisy environments. The Wiener filter was considered because of its applicability to situations where the signal and noise spectra shared a common frequency band and where the character of the signal could be estimated in advance of filtering. In practise other filtering techniques substantially isolated the signal and noise frequency bands and hence Wiener Filtering was not required. In this chapter we assess those Filter operators which were of practical use in the Elura environment.

6.2 Previous attempts at filtering

The principal shortcomings of the smoothing operations employed by Skrzeczynski and Meates (1977) Wilkes (1979), and Blackburn (1980) were that the operator was depending upon his subjective expectation of what the 'signal' component of the waveform should look like. Even with automatic smoothing by application of a running average, the operator had little or no idea what component of the noise spectrum was retained in

his smooth profile. This shortcoming was considered prohibitively serious in this study and the methods were accordingly avoided. They were however the methods in use prior to this study.

6.3 Upward Continuation

Experimented results for measured signal to noise ratios at different airborne elevations were reported by Spies (1978), Wilkes (1979) and Gidley and Stuart (1980). They observed that at a sensor elevation of about 100 metres the signal to noise ratio appeared to be greatest. Gidley and Stuart (1980) estimated that at this height the signal to noise ratio over the Elura orebody was about 12:1. In Fact they had no measure of the noise component contained in what they interpreted to be 'signal'. Thus the estimate of 12:1 must be considered as an upper limit.

In this study a measure of the noise component in the signal waveband was obtained from the spectrum of a signal free survey line. Elura line 50450N was used. The area under the curves in Figure 3.3 were used as a measure of signal at different elevations, while the area under the curves of Figure 4.1 gave a comparative measure of the noise. From these two sets of data, the best possible signal to noise ratios without filtering for airborne surveys could be derived. Further examination of Figure 3.3 and 4.1 confirm that filtering would only be effective for sensor elevations less than 50 metres because above this all the measured noise spectrum lies within the signal band width. This conclusion is important. The application of filtering to ground level data of course is important because the sensor is within 50 metres of the noise source.

The results of signal and noise energies at different sensor heights were tabulated in Table 6.1 and plotted in Figure 6.1. The latter figure contains plots of the rate of attenuation of the noise waveform from line 50450N (signal free) and the rate of attenuation of the signal derived from the Elura model. The rapid attenuation of the noise energy spectrum was expected and was the rationale behind the proposal to improve the signal to noise ratio by airborne surveying at the

TABLE 6.1: *Computed result of signal and noise energy spectra for sensor heights from 0.5 to 1000.5 metres*

Height above ground (m)	Signal energy spectrum ($nT^2/cy/m$)	Noise energy spectrum ($nT^2/cy/m$)	S/N ratio
0.5	13.93E+5	92.23E+5	0.15
5.5	12.95E+5	8.75E+5	1.48
10.5	12.06E+5	4.37E+5	2.76
20.5	10.49E+5	1.97E+5	5.32
30.5	9.14E+5	1.23E+5	7.46
40.5	7.99E+5	0.90E+5	8.90
50.5	7.01E+5	0.72E+5	9.70
60.5	6.16E+5	0.61E+5	10.06
70.5	5.42E+5	0.54E+5	10.08
80.5	4.78E+5	0.48E+5	9.94
90.5	4.23E+5	0.44E+5	9.66
100.5	3.75E+5	0.40E+5	9.31
200.5	1.22E+5	0.21E+5	5.71
300.5	0.46E+5	0.13E+5	3.40
400.5	0.19E+5	0.09E+5	2.13
500.5	0.09E+5	0.07E+5	1.38
1000.0	0.01E+5	0.02E+5	0.34

The signal energy spectra was computed for line 50850N from the known Elura orebody model.

The noise energy spectrum was calculated from field measurements from Elura line 50450N which was considered to contain noise only.

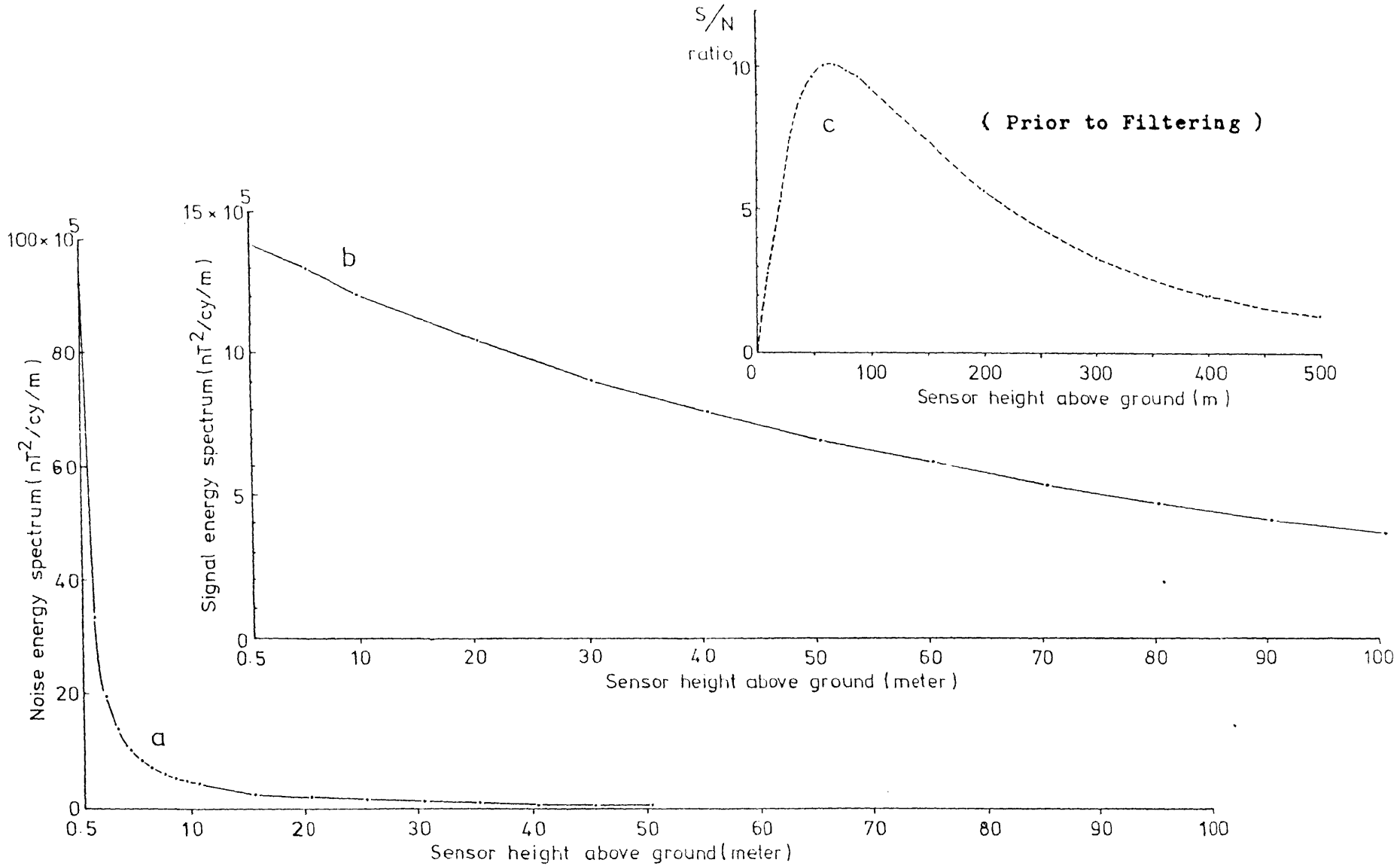

FIGURE 6.1: **a) & b) Plots of signal and noise against the sensor height above ground at Elura**
c) Signal/noise energy spectrum ratio.
a) and b) are respectively calculated from field data line 50450N prior to filtering and from the model of the known orebody.

appropriate elevation as proposed at the 1978 Symposium on applied magnetic interpretation. The attenuation with elevation of noise overlapping the signal band however could be seen from Figure 4.1 not to be as rapid as for the whole noise spectrum. This behaviour was predictable from the transfer function of the upward continuation filter.

The important conclusion from this data was that if an airborne survey was to be used then it should be flown at about 70 metres elevation at which the maximum signal to noise ratio over Elura would be 10:1. This result is in fair agreement with the observation of Gidley and Stuart but it identifies that about 20% of the 'Signal' interpreted by them was due to the low frequency component of the noise waveform.

Within the limitations of finite length of one dimensional input data, the application of the upward continuation filter to ground level data would approximate the result from an airborne survey. Thus, upward continuation cannot produce a signal to noise ratio any better than 10:1 in the Elura situation.

6.4 A Spike Rejection Filter

In accordance with the criterion defined in Chapter 5 section 8 for selecting a window and range for spike rejection, values of 200 data points and 100 nT respectively were chosen for the Elura data. The Figure 6.2 and 6.3 dramatically display the effect of spike replacement on the noise spectrum. Figure 6.2 shows the energy spectrum of a typical magnetic profile (Elura line 50450N) recorded over an area barren of deep mineralization but covered with a thin spread of maghemitic gravels. Figure 6.3 shows the energy spectrum of the same line after processing with the spike rejection filter.

In terms of the magnetic profile the effect of spike rejection was depicted in Figure 6.4 in which the raw and despiked data are plotted to the same scale.

The performance of the spike rejection filter was clearly demonstrated by these examples to be highly effective. The difficulties in properly using the filter as described in Chapter 5.8 and the

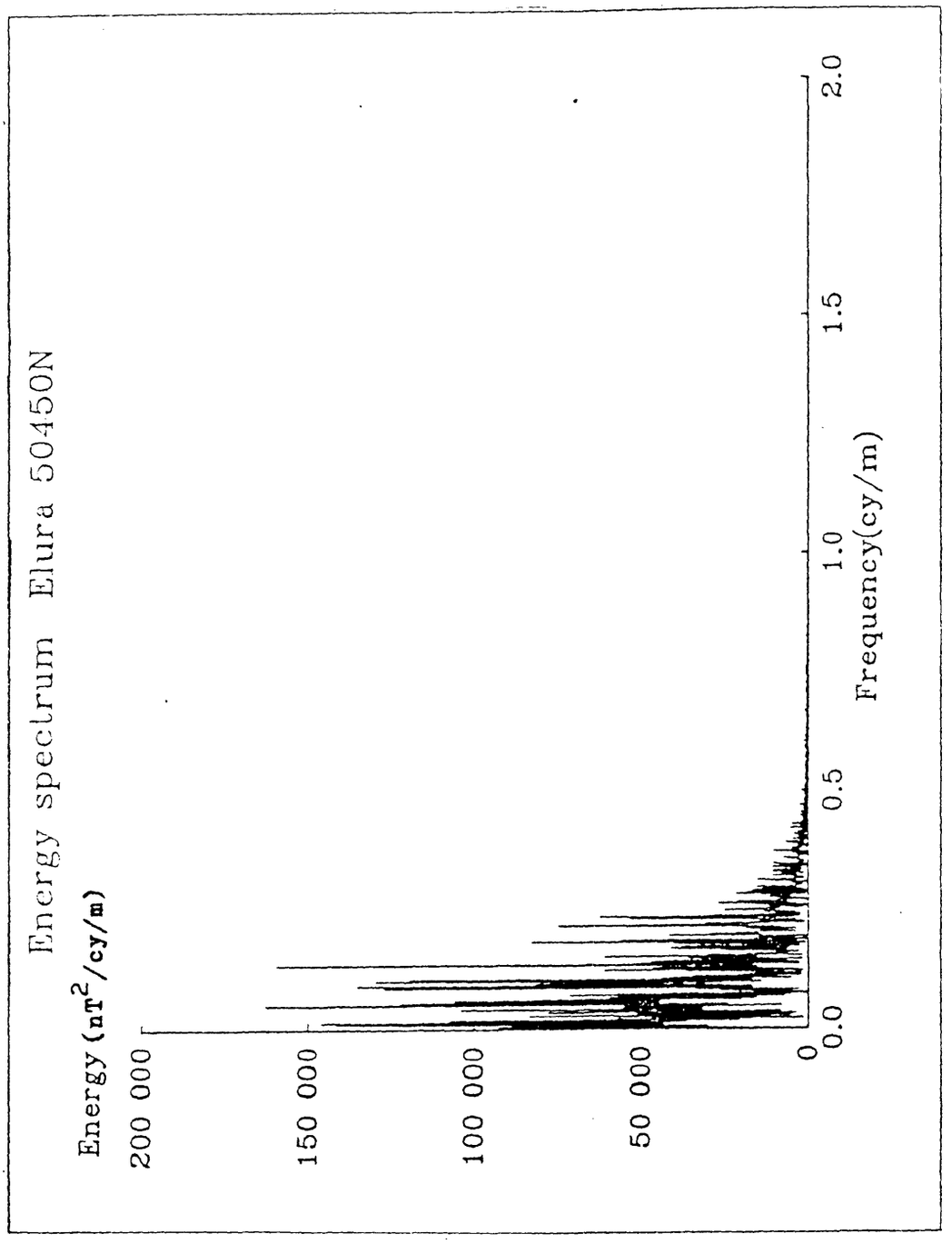

FIGURE 6.2: *Noise energy spectrum of the raw data, Elura line 5045ON.*

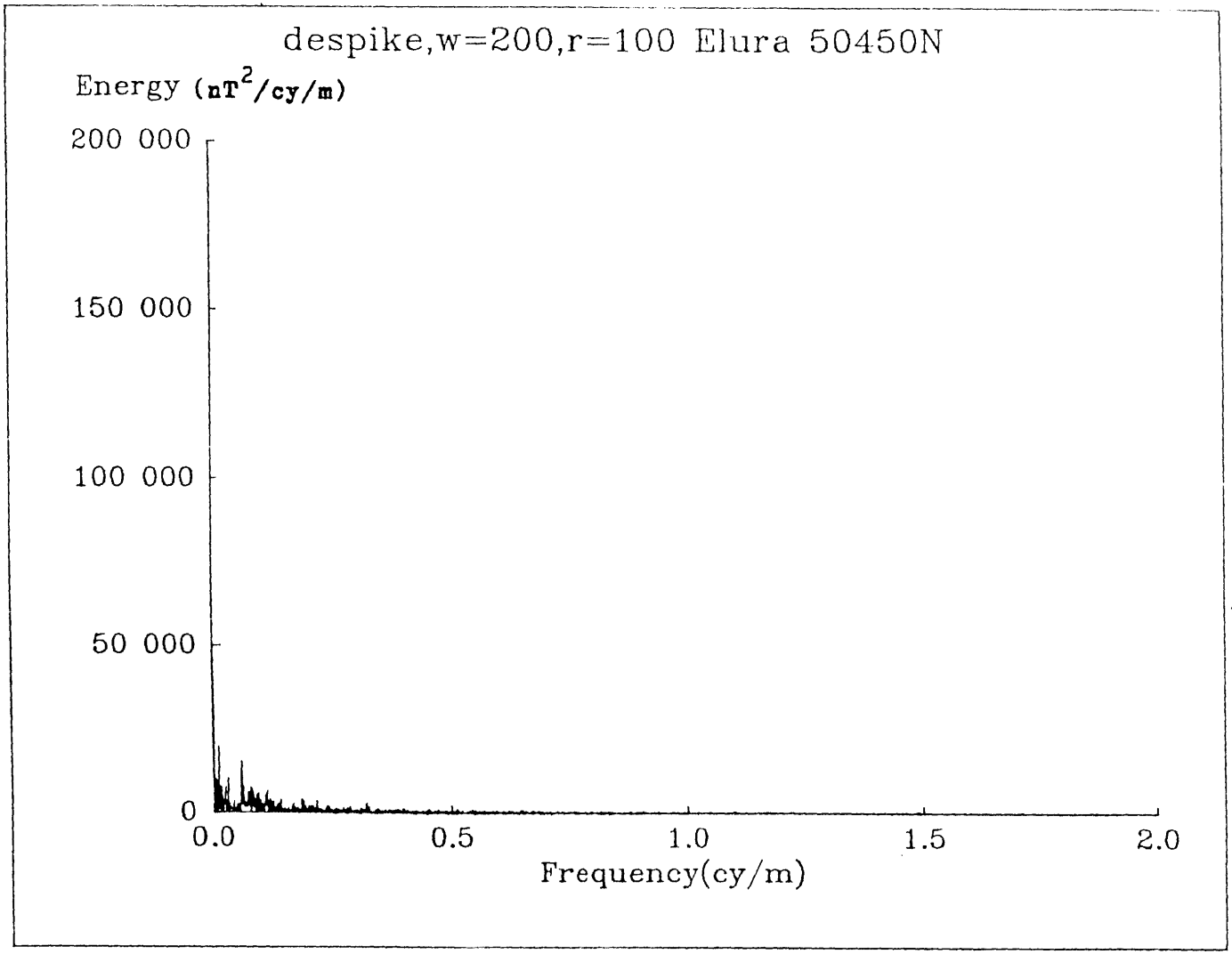

FIGURE 6.3: *Noise energy spectrum of Elura line 50450N after despiking.*

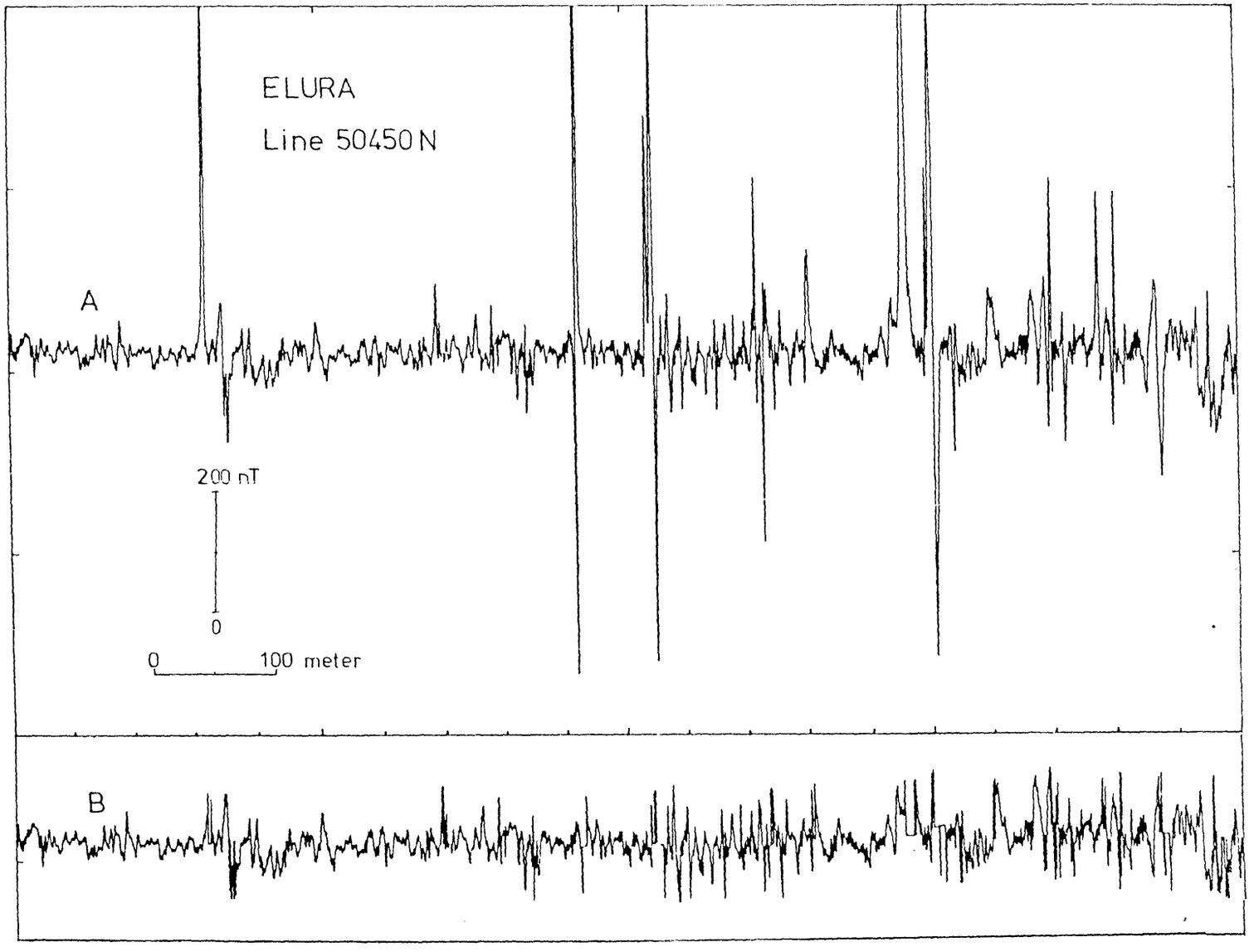

FIGURE 6.4: *Despiked profile in B with window length 200 points and range 100 nT from the raw data of the Elura noise profile in A*

inconvenience that the user need to monitor the behavior of the filter, were the main drawbacks of the program. Efficiency of computer CPU time confirmed this spike rejection routine to be preferable to median filtering.

6.5 A Median Filter

The median filter with a WINDOW of 101 data points was applied to two magnetic profiles from Elura. One profile was from line 50450N containing noise only and the other was from line 50850N containing both noise and signal. The computer CPU time required for each line was 5.6 minutes on a DECSYSTEM-20. The result of median filtering each of these lines was compared with both the raw data and the data processed with the Spike Rejection Filter of Chapter 5.8. Figure 6.5 and 6.6 respectively show the noise only and signal plus noise profiles. On first examination the median filtered data appears superior. Not only have spikes been removed but also a considerable amount of additional high frequency noise has been cleaned off. Close examination of the two processed profiles shows that the difference between the two is constrained to the high frequency end of the spectrum where linear low pass filtering would be effective. Thus, although the performance of the median filter on its own was superior to the Spike Reject filter, the combination of Spike Reject followed by low pass filtering would negate this superiority with much more economic use of computing time. (see Chapter 6.8)

6.6 The Filter of Spector and Grant

As detailed in Chapter 5.6, the filter of Spector and Grant is only a filter in the sense that it enables the spectral components of both signal and noise to be sufficiently separated as to be each identifyable. It does not enable the signal to be isolated from the noise in the spectral band where signal and noise overlap. Thus before applying this filter despiking by either the Median Filter or Spike Rejection Filter should be performed. The method of Spector and Grant was included here because it is a method commonly used for depth determination to the top of a source body and in the Elura environment it did not perform well even after despiking the raw data.

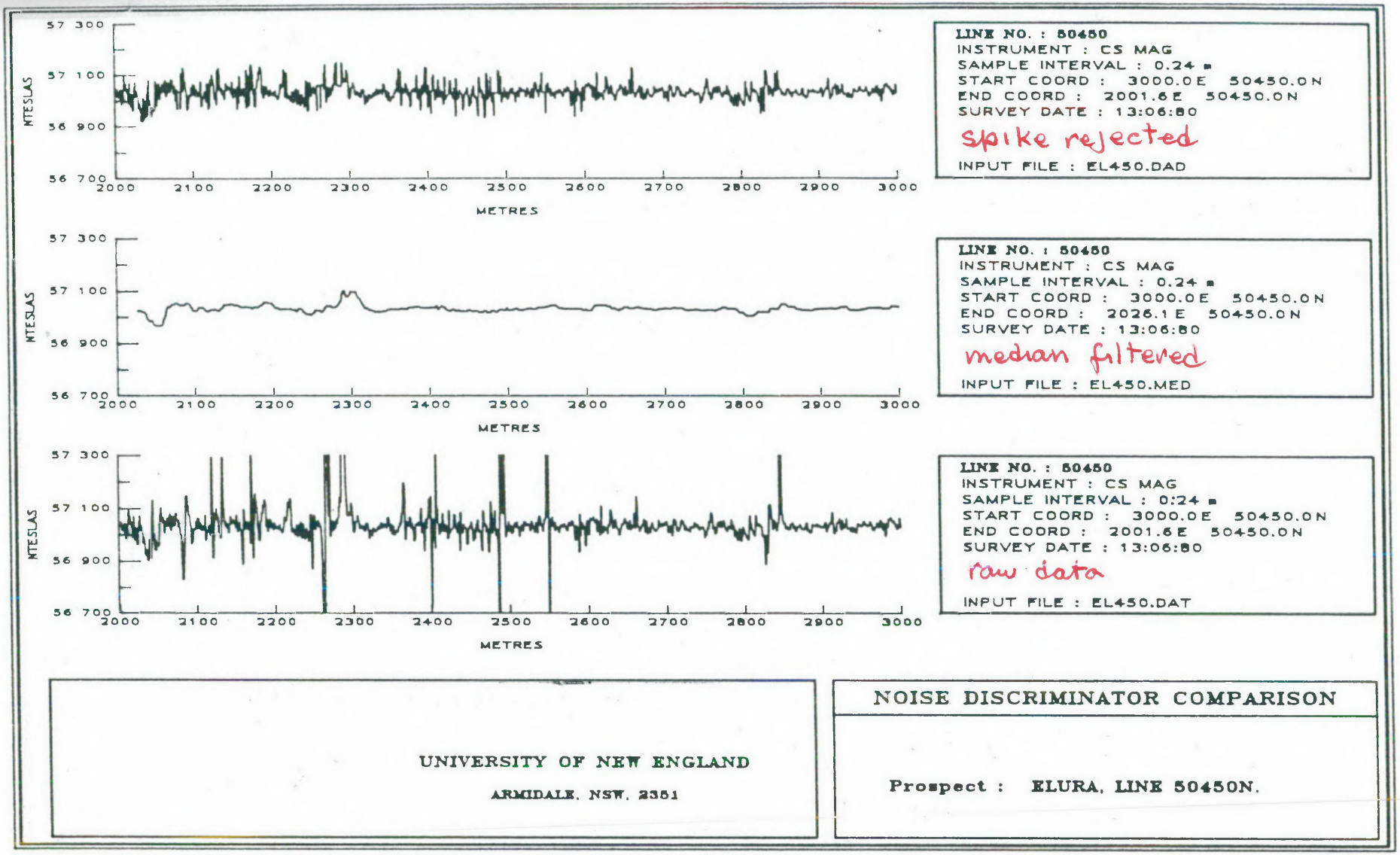

FIGURE 6.5: *A direct comparison between the raw data, median filtered data(W=101) and spike rejected data(W=100, R=100) for a noise only profile.* ~~(Label which profile is which. ie Raw Data, Median Filtered Data and Spike Reject Filtered Data)~~

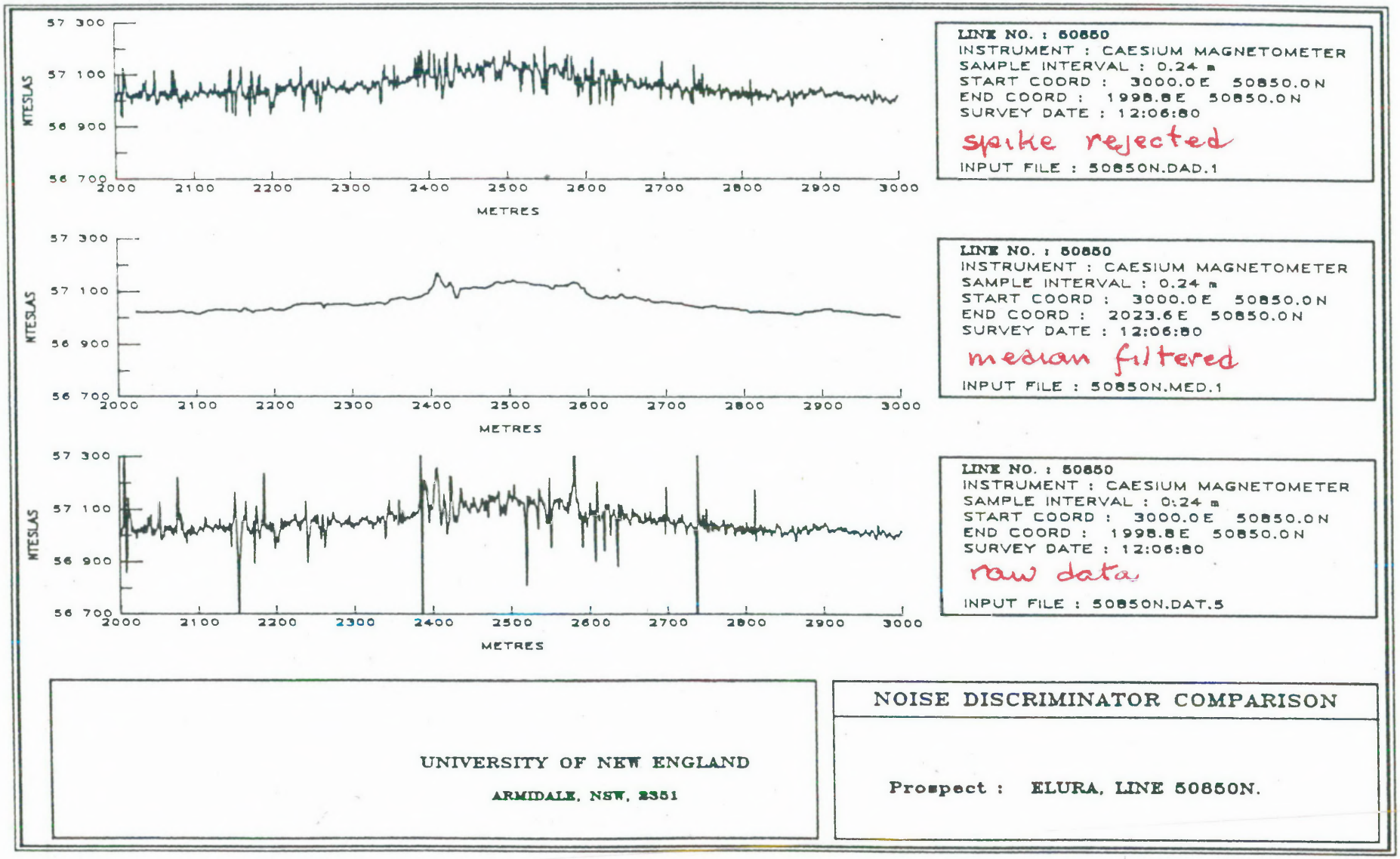

FIGURE 6.6: *A direct comparison between the raw data, median filtered data(W=101) and spike rejected data(W=100, R=100) for a profile containing both Signal and Noise.*

~~(Label which profile is which. ie Raw Data, Median Filtered Data and Spike Reject Filtered Data)~~

In Figure 6.7 the ln amplitude of the energy spectrum was plotted for Elura line 50800N after despiking the raw data. The slopes of two straight line segments were readily recognised and from them the depth to the top of the noise and signal source was calculated. The depth estimates however were overstated by a factor of about 5.

6.7 The Butterworth Filter

An attractive feature of the Butterworth Filter was its sharp and readily controlled cut-off as described in Chapter 5.4. The choice of cut-off frequency must be such that signal frequencies are passed with maximum rejection of higher frequency noise. The choice of cut-off frequency was therefore mainly dependent upon the signal source. Techniques for estimating the appropriate cut-off frequency for given signal sources are few. Gidley and Stuart (1980) applied Spector and Grants (1970) spectral factorization technique and determined a cut-off frequency point at 0.009 cycles/metre for the Elura data. Examination of the spectrum of modelled data from Elura revealed that 99.9% of the signal was contained below 0.005 cycles/metre and at 0.003 cycles/metre 94.8% of the signal was retained. These results were tabulated in Table 6.2 (See also Figure 3.2 and 3.3).

TABLE 6.2: *Percentage of signal cut-out from model data of the Elura line 50850N when filtering was performed with cut-off frequencies of 0.005 cycles/metre and 0.003 cycles/metre*

	Signal energy spectrum (nT^2/cy/m)	
	Filter cut-off (0.005 cy/m)	Filter cut-off (0.003 cy/m)
Model signal	13.93E+05	13.93E+05
Filtered model data	13.92E+05	13.20E+05
Signal cut-out	0.01E+05	0.73E+05
Percentage signal out	0.08	5.2

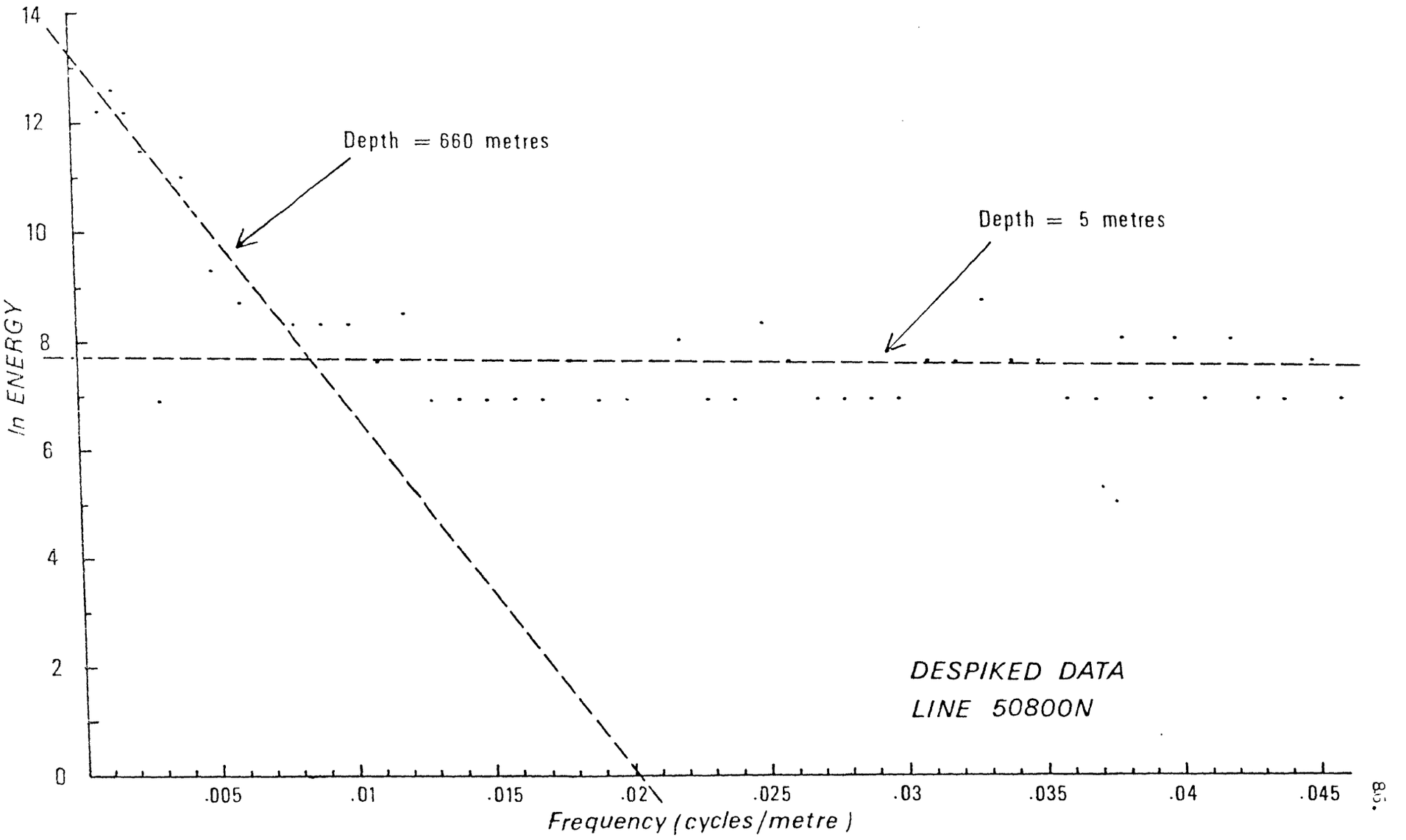

FIGURE 6.7: *The ln Amplitude energy spectrum of line 50800N after despiking. The method of Spector and Grant was used to estimate depths to the noise and signal source. The values obtained were overestimated by a factor of about 5.*

6.8 Combined Butterworth and Spike Rejection Filters

Having individually examined the Butterworth and spike Rejection Filters in relation to their performance at Elura it becomes apparent that a filter strategy in which Butterworth filtering was preceded by either spike Rejection or Median filtering would be optimum. For computing efficiency reasons the Spike Rejection method was adopted in preference to the Median Filter. In this section the percentage of signal cut-out and the percentage of noise left in were calculated for combined Spike Rejection and Butterworth Filtered data in order that a figure for achieved signal to noise ratio could be derived. The calculation was performed for data from Elura line 50850N.

Total signal energy spectrum of the model Elura line 50850N was 13.92579E+05 $nT^2/cy/m$. With the cut-off frequency at 0.005 cycles/metre, the signal energy spectrum cut-out was 0.01119E $nT^2/cy/m$ or 0.08%, see Figure 3.2 and Table 6.2. With a cut-off at 0.003 cycles/metre,the percentage signal filtered out was 5.2%.

When the noise profile (Elura 50450N) was despiked and filtered at 0.005 cycles/metre,the energy of the spectrum still remaining below 0.005 cycles/metre was 0.28792E+05 $nT^2/cy/m$, which is 2% of the Elura orebody signal. With a filter cut-off of 0.003 cycles/metre, the value was 0.85% (Table 6.3).

It can therefore be concluded that the optimum filter cut-off frequency applicable to the Elura orebody is between 0.005 and 0.003 cycles/metre with the latter leaving less noise energy, but removing some of the signal. In both cases, the error due to noise or due to distortion of the signal amounts to about 2%.

The same procedure for establishing the signal to noise ratio for filtered and despiked data was used to investigate the relationship between signal to noise ratio achievable after filtering and the height of the sensor above ground at low levels. (c.f. the results obtained for high levels, Chapter 6.3). The results of this investigation were tabulated in Table 6.4. Quite conclusively, the signal to noise ratio dramatically increases as the sensor approached ground level from about 6 metres. However, at elevations of less than 1.5 metres the rate of

TABLE 6.3: *Noise left in after despiking and filtering for Elura line 50450N, expressed as a percentage of the Elura signal at line 50850N*

	Energy spectrum (nT^2/cy/m)	
	Filter cut-off (0.005 cy/m)	Filter cut-off (0.003 cy/m)
Total signal energy - Elura line 50850N	13.93E+05	13.93E+05
Noise left after despiking + filtering	0.29E+05	0.12E+05
Noise left in as percentage of signal	2.1	0.85

TABLE 6.4: *Signal-to-noise ratio results of the despiked and filtered Elura lines 50850N and 50450N for the sensor heights from 0.5 to 5.5 metres*

Height above ground (m)	Signal energy spectrum (nT^2/cy/m)	Noise energy spectrum (nT^2/cy/m)	S/N ratio
0.5	13.92E+05	0.29E+05	48.4
1.5	13.79E+05	0.29E+05	47.6
2.5	14.62E+05	0.46E+05	31.9
3.5	15.28E+05	0.76E+05	20.0
4.5	16.36E+05	1.29E+05	12.7
5.5	14.15E+05	2.19E+05	6.5

The signal-to-noise ratio is maximum when the sensor is very near the ground surface.

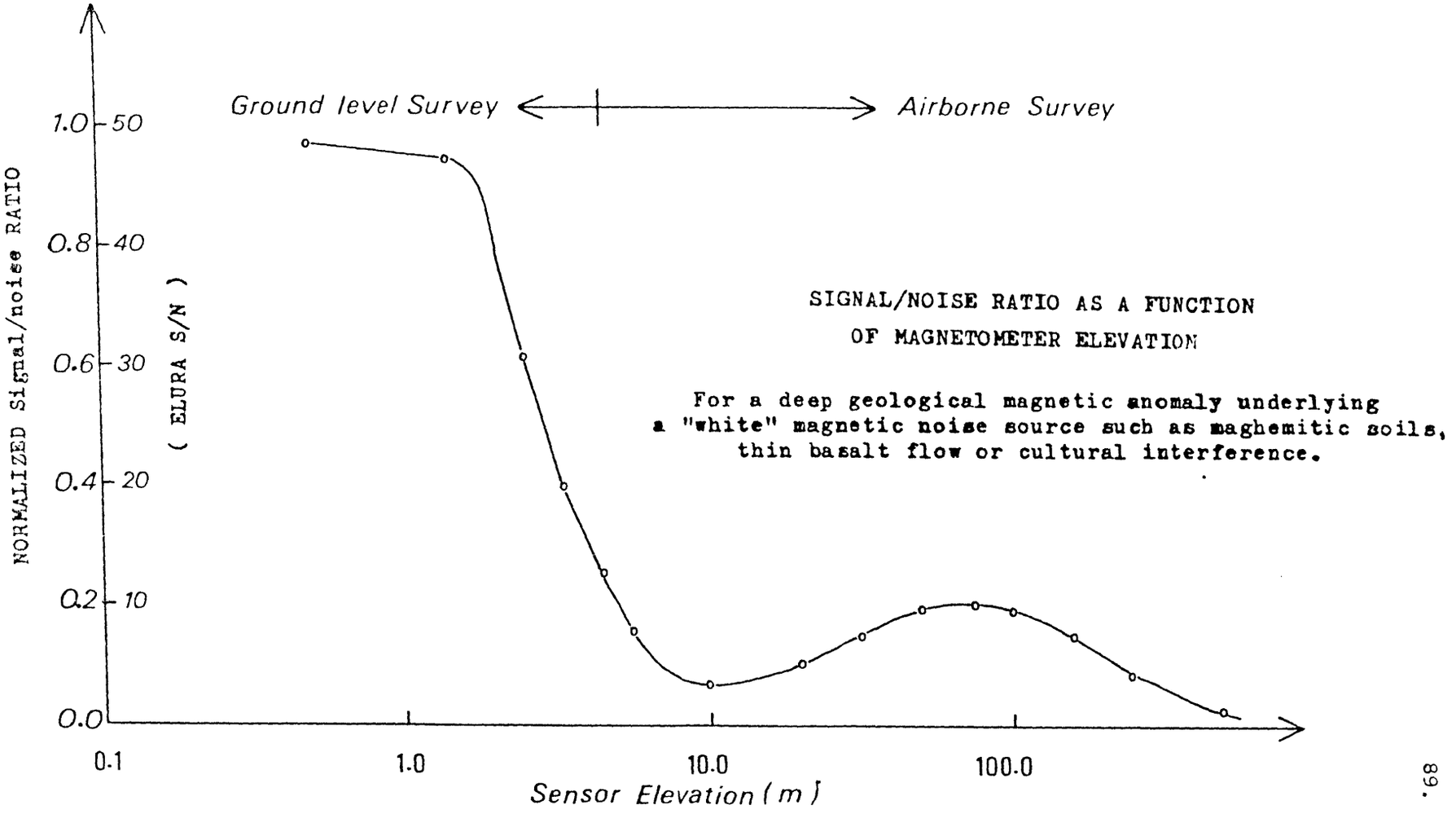

FIGURE 6.8: *A plot of the maximum signal to noise ratio achievable at different sensor elevations after filtering. (Elura situation).*

improvement decreased. Considering the logistics of data sampling close to a noise source where the sample interval was shown (Chapter 4) to have to approximately equal the sensor elevation, then the logical compromise was to sample the data at about 1.5 metres above ground with a sample interval of 2 metres. This was considered to be one of the more important conclusions of this study. The achieved signal to noise ratio of 48:1 was also considered important because of its significant superiority to that achieved by an airborne survey. Thus the stated objective of defining the relative performance of ground level versus airborne surveying in areas of intense ground noise was achieved.

In Figure 6.8 was plotted on a semilog scale the maximum signal to noise ratio after filtering, achievable at different sensor elevations from 0.5 metre to 500 metres above the Elura orebody.

The form of this curve will be general for areas where the surface noise is of similar character to that at Elura, ie broad band. The effect of a different signal amplitude or noise amplitude will only be to alter the vertical scale factor. For this reason the vertical axis has been normalized as shown.

6.9 Conclusion

It can be concluded that if an airborne survey was to be used then the sensor elevation should be at about 70 metres to obtain maximum signal to noise ratio. The maximum signal to noise ratio at this sensor elevation ~~moved~~ obtained by upward continuation would be 10:1.

For ground survey with filtering, filtering would only be effective for the sensor elevation less than 50 metres since the above this all the measured noise spectrum lies within the signal band width. Butterworth filtering which was preceded by either Spike Rejection or Median Filtering would be optimum. For computing efficiency reasons the Spike Rejection method was adopted in preference to Median Filter. With this filtering technique to the very low sensor elevation data, the maximum signal to noise ratio is 48:1 which is very much better than airborne survey.

By applying this filtering technique to the Elura case study area, its excellent result will be shown in the next chapter.

Chapter 7

RESULT FROM THE ELURA CASE STUDY AREA

7.1 Introduction

The Elura orebody has now been extensively drilled and its dimensions and composition are quite well known. Because of this it can be modelled and the theoretical data compared with that achieved after processing the ~~procession~~ measured magnetic data. The environment around the orebody was not so well known in that it has not been drilled. The extensive geophysical case study programs that were conducted over Elura before mining commenced did not do more than confirm, to varying degrees of success, the existence of the already known orebody. In the absence of further targets being revealed by such intensive geophysical study it is not surprising that further exploratory drilling was not conducted.

In this chapter we present all the processed caesium magnetometer data from the Elura grid, identify the anomaly arising from the known orebody and then take a closer look at what additional information was revealed as a consequence of this improved data quality.

The application of this study was then extended to the situation of exploration beneath maghemitic palaeochannels and to a determination of depths and sizes of theoretical exploration targets which would be detectable using high resolution ground magnetics in an Elura environment.

7.2 The Elura Survey Results

After processing the field data as described, it was presented as a contour map in Figure 7.2. With the signal to noise ratio of 48:1, this map contains far higher quality and resolution data than had previously been obtained.

In Figure 7.3 the same data was presented in a pseudo perspective format.

Analogue profiles of the individual survey line data have been included in Appendix I.

7.3 Interpretation of the Elura Data

Detailed interpretation of the data in terms of defining the source geological structure was not an objective of the study. However with the significantly improved quality of the data, some information about the structure surrounding the known orebody could be derived.

Modelling of the known orebody was considered to be of little more use than to offer a broad check that something fundamental was not wrong with the signal to noise investigation about which this study was concerned. Irregularities in the fit of modelled data to the processed field data could equally be attributed to inadequacies of the input model data as to the field data. In Figure 7.4 however a single line comparison was made between data from a relatively simple model of the known orebody (see Figure 3.1) and the processed data. It can be seen that the fit is good except for small flanking anomalies in the field data which did not appear in the model. The most reasonable explanation of this variation between model and field data lies in the probability of a magnetic halo around the contact of the orebody which was not reported in the description of the orebody mineralogy.

In addition to the anomaly associated with the known orebody another significant, similar anomaly was resolved to the north. (See Figure 7.1). The amplitude of the second anomaly was about half that of the main anomaly. In cross section however the two anomalies showed a resemblance in that each displayed a dominant central peak and each was

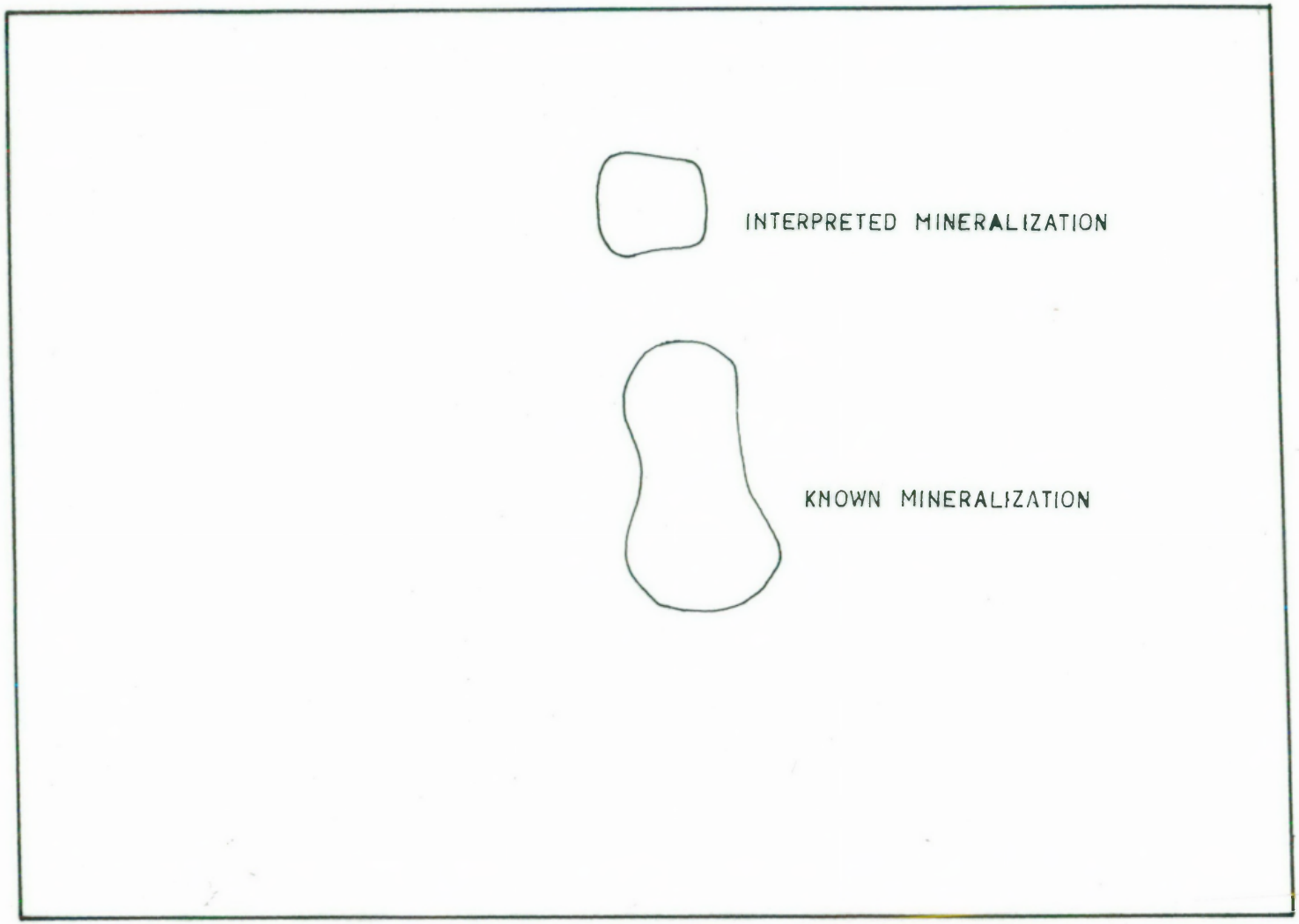

FIGURE 7.1: OVERLAY SHOWING THE PROJECTED POSITION OF THE KNOWN MINERALIZATION AND THAT OF INTERPRETED MINERALIZATION.

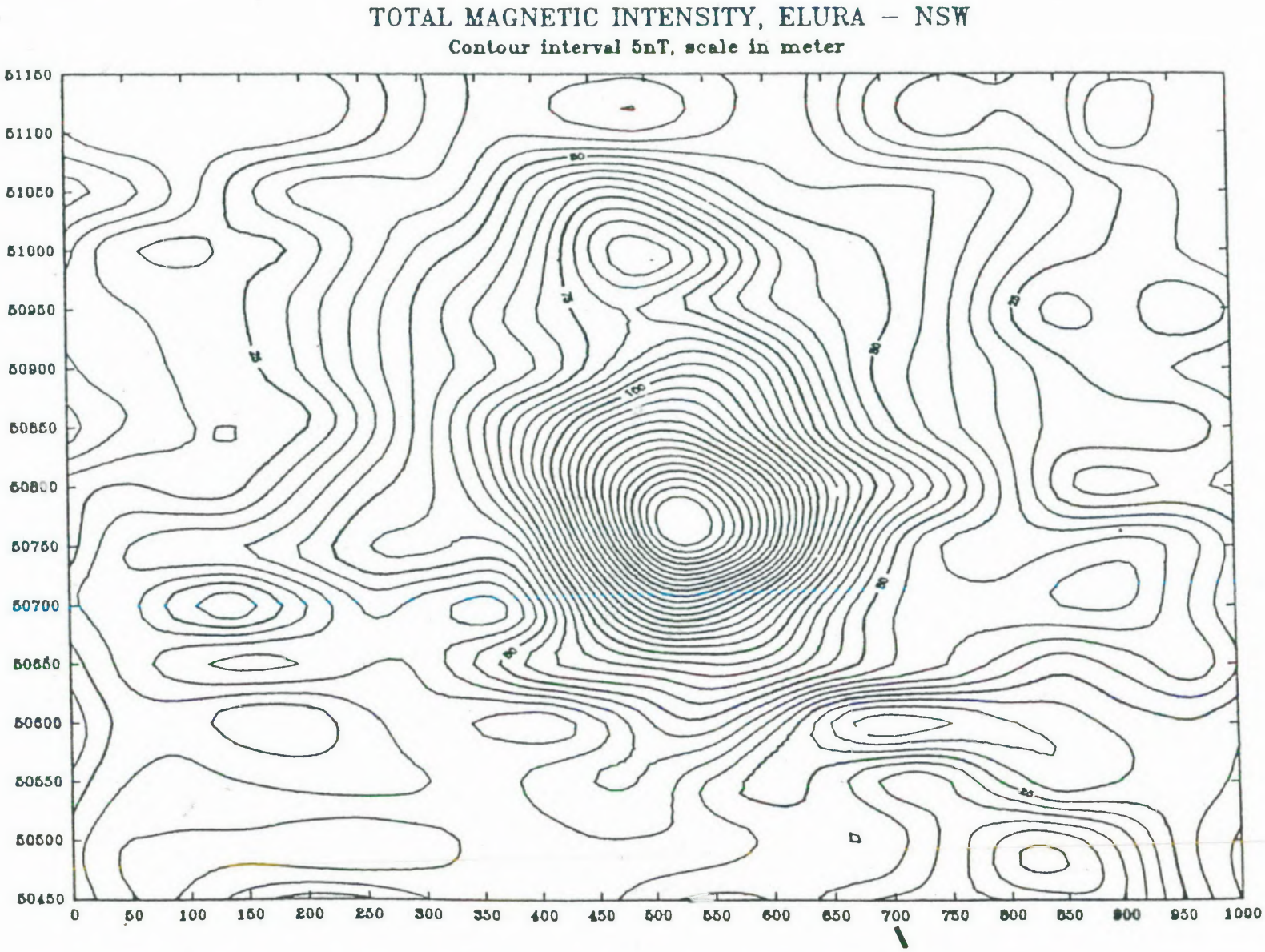

FIGURE 7.2: *Contour map of the processed magnetic survey data. The signal to noise ratio of this data was determined to be* 48:1.

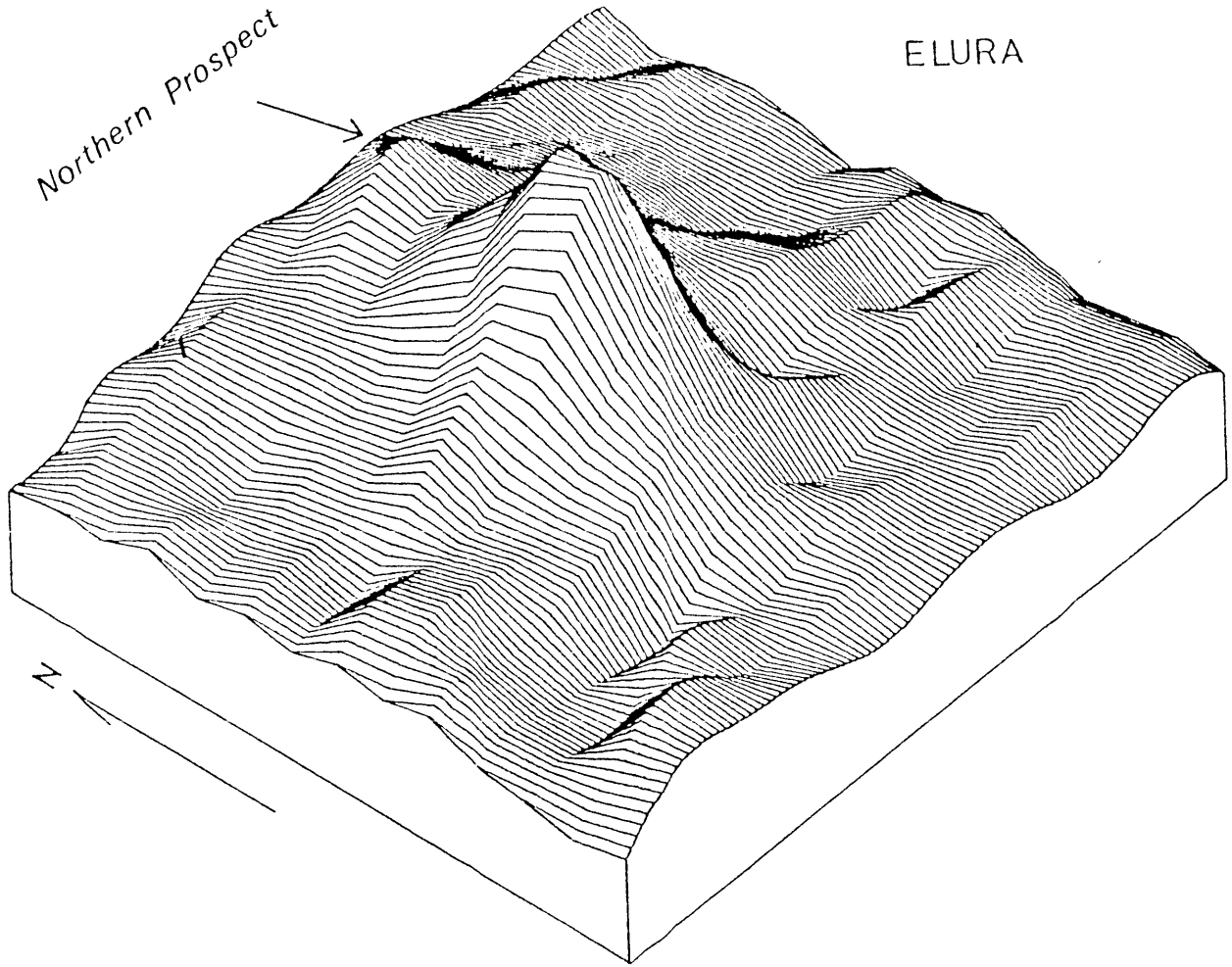

FIGURE 7.3: *Elura Zn-Pb-Ag anomaly with a newly discovered anomaly in the northern part of the Elura orebody.*

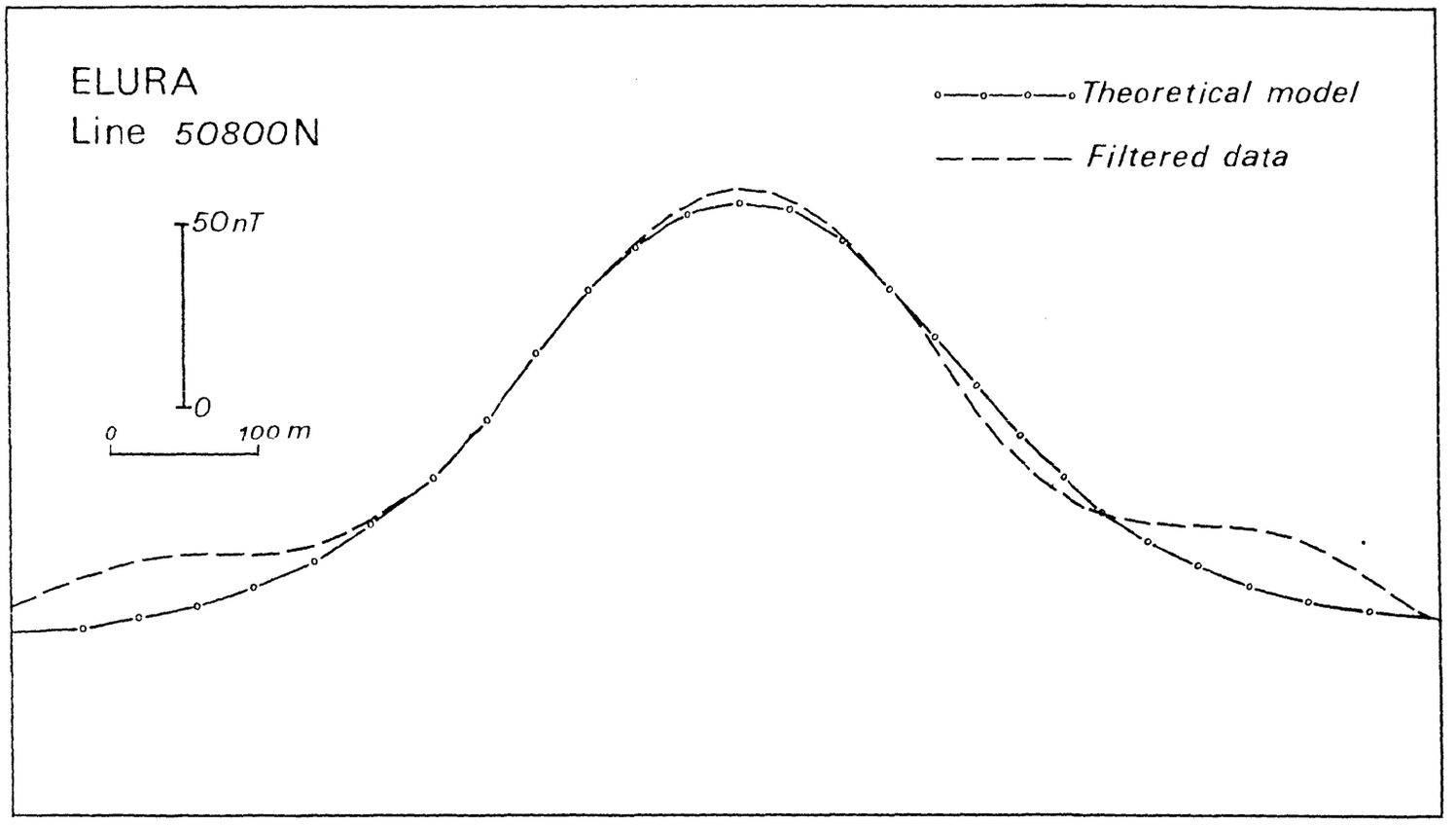

FIGURE 7.4: *A comparison between modelled data and processed field data corresponding to line 50800N. Note the small discrepancy on either flank of the main anomaly. These were interpreted as arising from a magnetic halo about the main mineralized zone.*

flanked by a minor shoulder. The northern anomaly was modelled as a prismatic body of dimension 60 metres (north-south) by 80 metres (east west). The depth to the top of the body was 150 metres and its thickness at least 400 metres. A susceptibility of 0.0088 gave the fit pictured in Figure 7.5. The similarity between the interpreted susceptibility of the northern anomaly and that of the pyrrhotitic zone of the main orebody further suggest a similarly in composition of the two sources. The composite model of the two bodies was represented in Figure 7.6. While we debated at length the possibility of faulting controlling the original mineral emplacement and/or later separation of the inferred body from the known orebody, it was finally decided that insufficient evidence was visible to propose such faulting.

7.4 Theoretical Exploration Targets detectable in the Elura Environment

A model Elura body with dimensions the same as in Figure 3.1 of Chapter 3, was set at depths from 50 to 600 metres below the magnetic sensor and the corresponding signal spectra computed. The Elura line 50450N was again chosen as a representative noise profile. The noise energy spectrum after filtering at 0.005 cycles/metre cut-off was computed to be 0.28790E+05 nT^2/cy/m and the signal energy spectrum for each depth listed in Table 7.1 and plotted Figure 3.3. The signal amplitude and the signal-to-noise ratios at each model depth were computed and were shown in Table 7.1 and Figure 7.7.

From Figure 7.7 and our knowledge now of the noise energy remaining after processing, for data from several sensor elevations, we can deduce the depth to which a signal from a target of given size and magnetic susceptibility could be detected beneath a predicted intensity of noise. As a very conservative criterion for the detection of a signal, it was proposed that the signal to noise ratio must exceed 5:1. Under ideal close-grid conditions where the anomaly has been traversed by several adjacent survey lines this ratio could be reduced to 1:1. In the case of the Elura orebody in the Elura noise environment, the signal to noise ratio for a ground level survey was predicted to exceed 5:1 had this body occurred at any depth down to 280 metres. Using the more optimistic 1:1 ratio criterion, the Elura orebody would remain detectable to 475 metres.

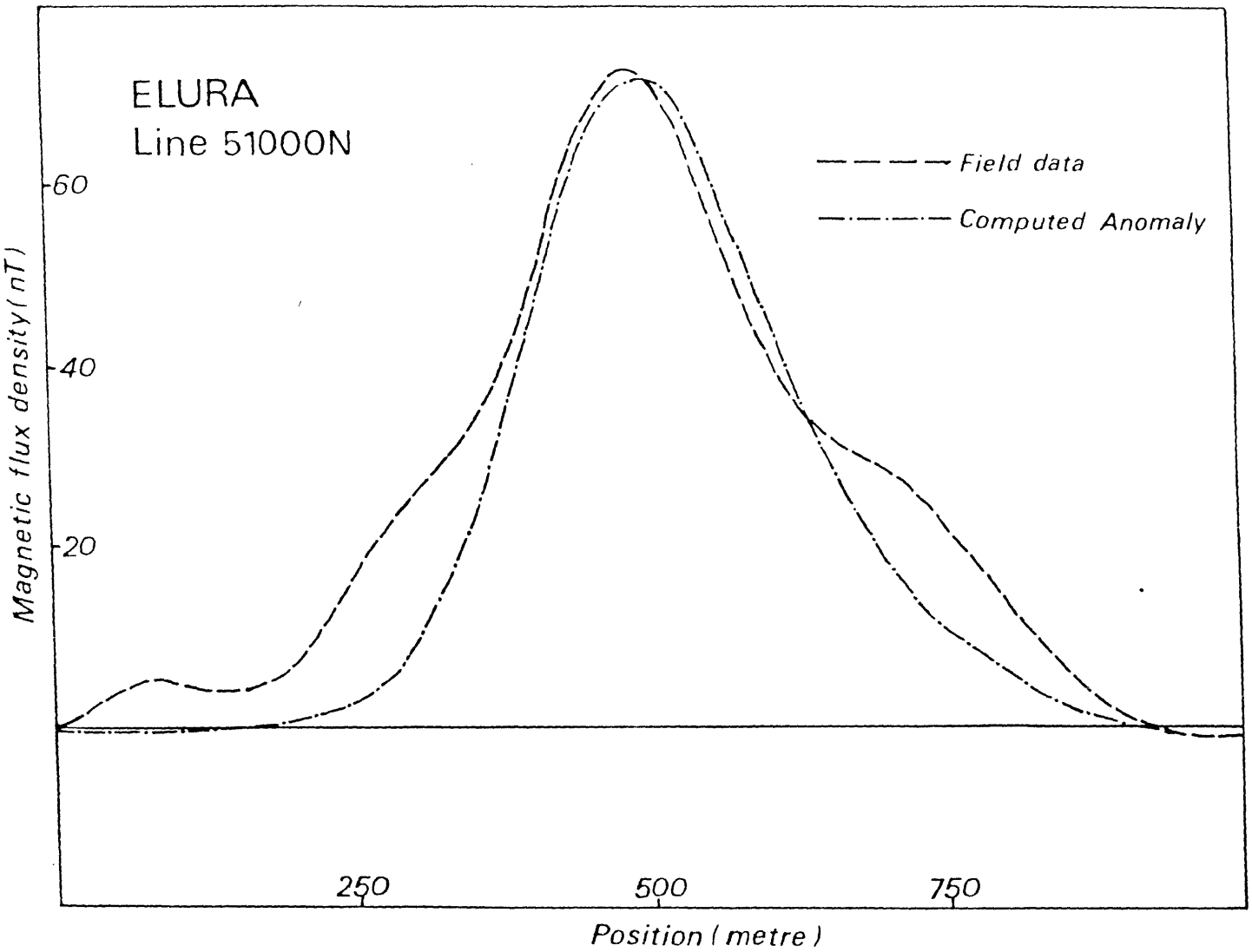

FIGURE 7.5: *Theoretical computed magnetic anomaly to the north of the known orebody. The dimension of the model were presented in the text.*

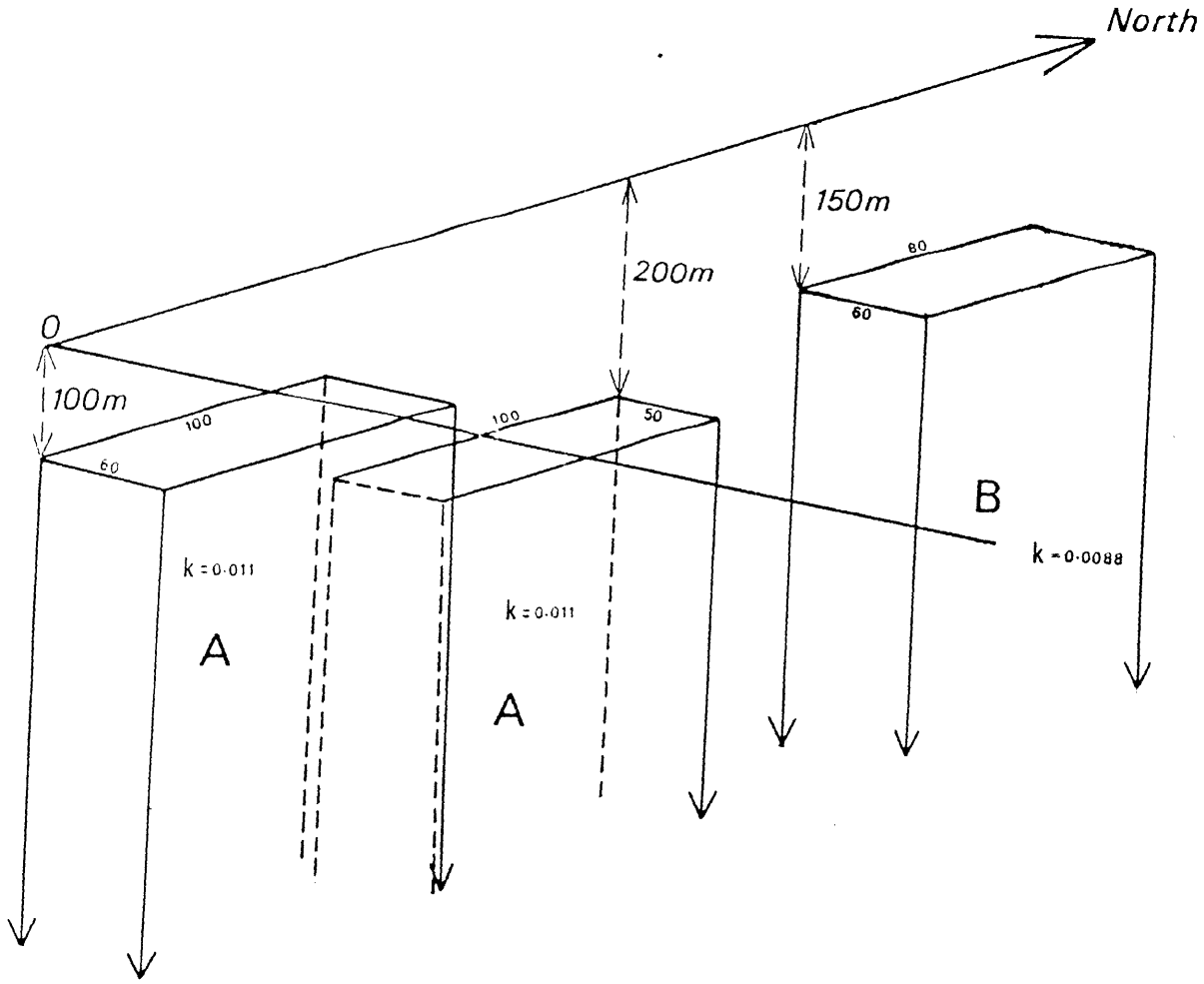

FIGURE 7.6: *Schematic representation of the model of the pyrrhotitic component of the known mineralization (A) and the inferred body (B) to the north.*

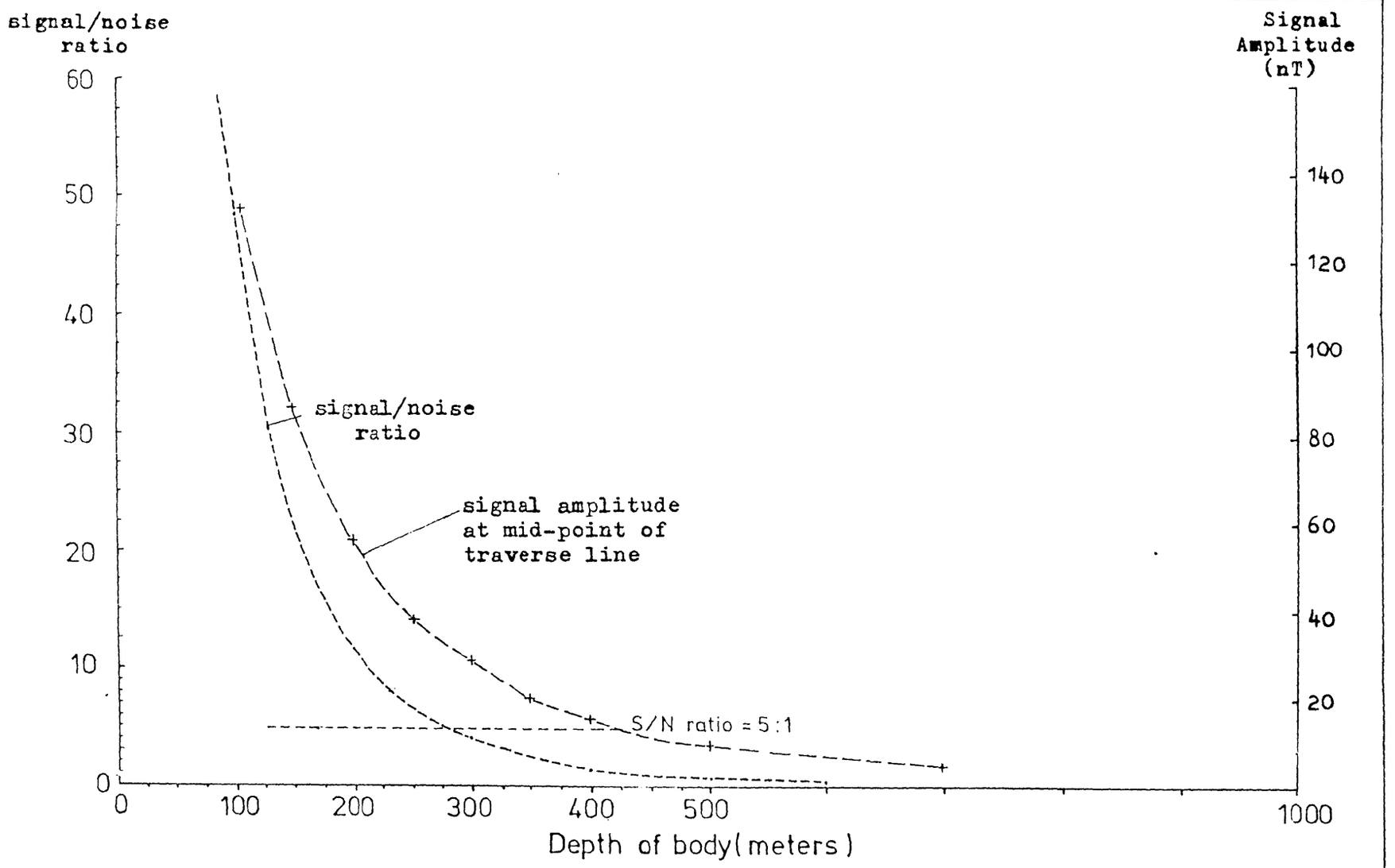

FIGURE 7.7: **Plot of signal/noise ratio and signal amplitude of the Elura model body line 50850N at different depths for a ground level magnetic sensor.**

The optimum elevation airborne survey at 75 metres would yield a signal to noise ratio greater than 5:1 for an Elura orebody source down to a depth of 155 metres. If the flight line spacing were 100 metres or less, then the body could have been detected down to a depth of 300 metres with a signal to noise ratio greater than 1:1.

In the worst case of a helicopter survey at 10 metres elevation Elura could only have been detected had it existed within 40 metres of the surface (5:1 ratio) or 165 metres (1:1 ratio).

In order to investigate the depth to which bodies similar to Elura in composition, but different theoretical tonnages a square prism model was assumed. The dimensions were defined such that the width was always equal to one-fifth of the depth extent. By varying the dimensions and the depth of cover below the ground surface, a set of anomaly curves were computed corresponding to different orebody tonnages at different depths. The magnetic susceptibility of the bodies was defined

TABLE 7.1: *Computed signal-to-noise ratios for the Elura model body at different depths*

Depth (metres)	Signal energy spectrum (nT^2/cy/m)	Signal-to-noise ratio
50	23.94E+05	83.2
100	13.92E+05	48.4
300	1.22E+05	4.2
400	0.46E+05	1.6
500	0.19E+05	0.7
600	0.09E+05	0.3
1000	0.01E+05	0.0

Noise energy spectrum is from the filtered Elura line 50450N.

Noise energy spectrum = 0.287790E+05 nT^2/cy/m.

consevatively as 0.0035 S.I. units (The Elura model was 0.011) and the body density was assumed to be 4.2 gm/cc. The energy spectra of each of the anomaly curves were calculated. Assuming the noise energy of 0.28790E+05 $nT^2/cy/m$ derived from line 50450N, the signal/noise ratic for each anomaly curve was obtained.

Figure 7.8 shows a plot of the signal/noise ratio for each of 5, 10, 20, 30 and 50 million tonne bodies at depths down to 1000 metres. Again the very conservative signal/noise ratio of five was adopted as the value above which the magnetic signal would be recognizable.

7.5 Exploration beneath maghemitic palaeochannels

The existence of maghemite palaeochannels has presented extreme problems to geophysical exploration. The intense magnetization and high electrical conductivity of the channels have been considered sufficient to mask any deep source anomaly that may be of exploration interest. For this reason, regions cut by palaeochannels have previously been left unexplored by geophysical methods.

In this study of the application of filtering techniques to magnetic data from areas of maghemite occurrence, the maghemite palaeochannel provided the ultimate test of the processing strategy. Data was recorded across a palaeochannel chosen as representative of the most magnetic examples encountered in the Cobar region. There was no deep magnetic source known to underlie the channel. The Spike replacement processing program was applied to the data before Butterworth filtering. The residual waveform was used to assess the performance of the processing stategy.

A maghemitic palaeochannel overlying an area of no known deep magnetic source was selected from the Elura South area. The channel dimensions were determined from auger drill profiles recorded by Newmont Holdings Pty Ltd as part of a geochemical sampling program. A cross section of the channel along survey grid line 8400N was presented in Figure 7.9. The orientation of the channel was north-south. As seen from the cross-section, the channel varied from 0.25 to 2.5 metres thickness containing concentrated maghemite gravels. The depth to the top of

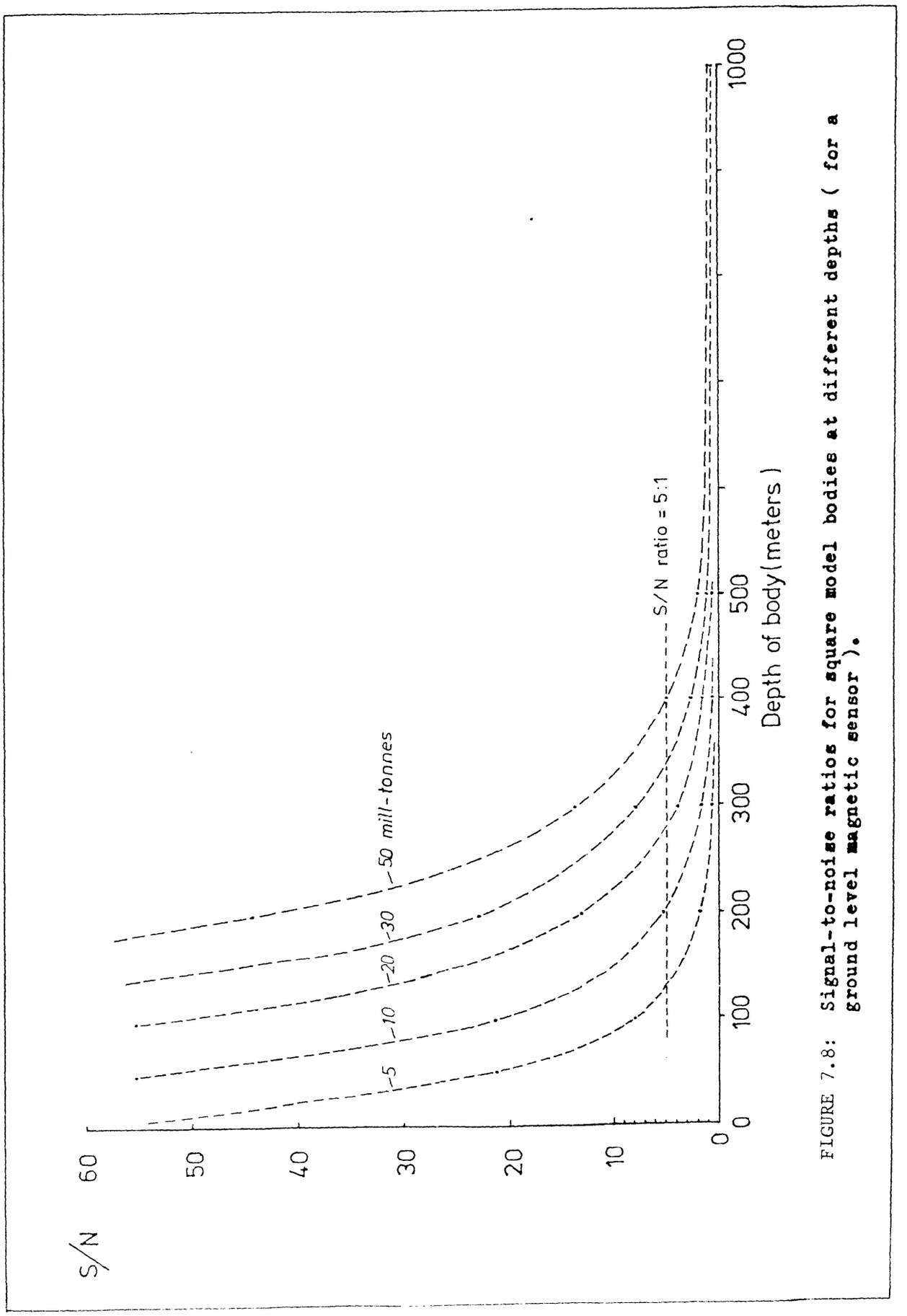

FIGURE 7.8: **Signal-to-noise ratios for square model bodies at different depths (for a ground level magnetic sensor).**

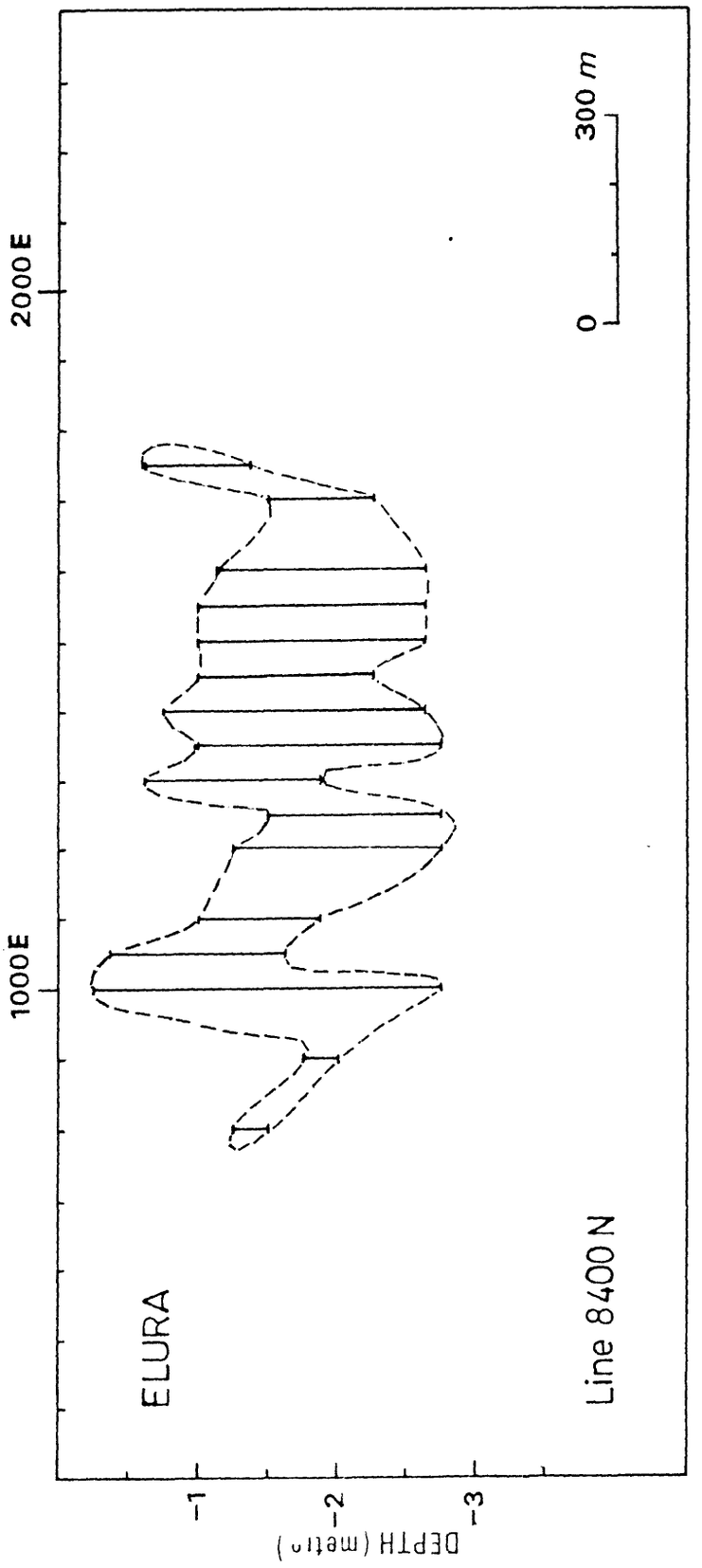

FIGURE 7.9: *A cross section through a well developed maghemitic palaeochannel as determined from auger drilling at the location indicated.*

the channel was typically less than 1 metre and its width approximately 800 metres. This channel represented the worst possible case for magnetic exploration for a deep target because of its magnetic intensity and width of influence.

The raw data was plotted in Figure 7.10 Superimposed on that Figure was the magnetic profile resulting from processing the raw data with despike program (window 200 data points, Range 100 nT) followed by low pass Butterworth Filtering with a cut-off frequency of 0.005 cycles/metre. The resulting profile (assuming the absence of a deep magnetic source) was considered to consist of a sum of the net induced component magnetic anomaly arising from the anomalous 'Slab model' (representing the palaeochannel) plus the residual contribution to the long wave length spectrum arising from the extremely intense remanent magnetization of the maghemite gravels. Attempts to model the induced component of the cnannal anomaly were unsuccessful as the magnetic profile was dominated by the unpredictable remanent magnetic component. However, as can be seen from Figure 7.10 the peak to peak wave form envelope after processing was of the order of 50 nT. Thus it can be concluded that if the chosen example line 8400N, was representative of a typical 'noise only' profile over a maghemitic channel any deep source anomaly of amplitude significantly greater than 50 nT would be recognizable if it were covered by several survey lines. (criterion of signal to noise ratio of 1:1) To be recognized from a single survey line the 5:1 criterion would require a signal anomaly amplitude of 250 nT. It was then concluded that had the Elura orebody existed beneath such a channel then it could have been detected from a ground level survey at any depth down to 25 metres (5:1 ratio) or 160 metres (1:1 ratio). The optimum elevation airborne survey at 75 metres could not detect the body at any depth with a signal to noise ratio greater than 5:1 and it could only detect it to a depth of 55 metres with a signal to noise ratio greater than 1:1. A survey flown at 10 metre elevation could not detect the body at all.

It should finally be noted that while only one line (8400N) was given here as an example, some 40 lines were surveyed at a spacing of 200 metres following this channel. Of these, line 8400N was considered to be amongst the worst cases.

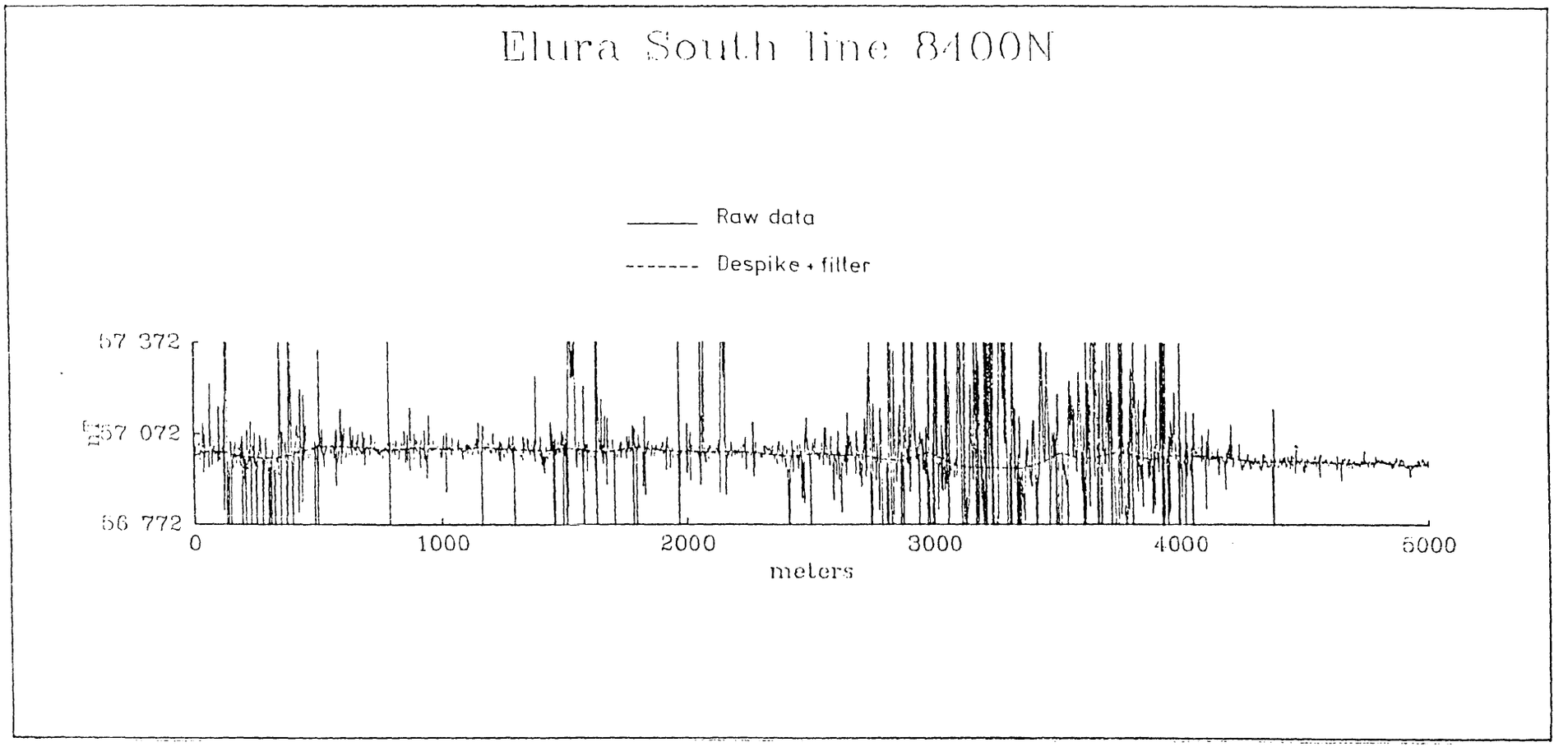

FIGURE 7.10: *Raw and filtered data of the Elura South line 8400N. Filtered data are fitted to the raw data. A maghemite channel existed between 2750-4000 metres. The envelope of the filtered data was approximately 50 nT.*

7.6 Conclusion

By applying the filtering techniques to the Elura magnetic data, the result shows that there is a newly discovered prospect in the northern part of the Elura orebody.

From the data presented, we can make estimate of the maximum depth of burial at which orebodies of different sizes might be expected to be located magnetically using the proposed survey and filtering technique. The composition of the body was assumed to be similar to the Elura orebody and the cirterion adopted for positively identifying the magnetic signal anomaly from a single profile was a conservative signal/noise ratio of five.

Chapter 8

CONCLUSION

The problems associated with magnetic exploration in areas covered by a near surface source of magnetic noise such as concentrations of maghemitic mineralization, thin basalt flow or cultural magnetic objects have long been recognized. Attempts that have been made to suppress noise interference by either using airborne surveying to distance the sensor from the noise source, or by the application of smoothing operators to data recorded as far above the ground as practical using hand carried magnetometers. In both cases the method of assessing the merit of the procedure was subjective being based upon the observed smoothness of the residual anomaly. In fact there was no measure of the amount of signal energy that was rejected by the procedure or the amount of noise energy that was accepted, because the two could not be quantitatively distinguished. In most previous studies the amount of noise energy folded back into the signal spectrum due to undersampling was unknown. In this study the spectra of near surface sources of noise were defined, the spectra of typical target signals and that from the Elura orebody in particular, were defined, and a quantitative study of sampling and signal processing was achieved. The effects of filter operators and the elevation of the magnetic sensor above the noise source could then be quantitatively investigated.

The principle conclusions of this quantitative analysis were then summarized as follows:

1. Surface concentrations of magnetic iron oxide minerals, thin basalt flow and scattered magnetic cultural artifacts provided near surface noise sources which were spectrally broad band.

2. Broad band or "white" noise sources required sampling at an interval approximately equal to the sensor elevation above the source if aliasing greater than 1% were to be prevented.

3. As a consequence of its broad band nature, the spectrum of a white noise source must overlap that of a signal and therefore it cannot be completely separated by linear filtering. In particular, upward continuation filtering either by computation or airborne surveying was not capable of removing that component of the noise spectrum which overlapped the signal spectrum.

4. A nonlinear filter which recognized a noise waveform in ground level survey data by its high frequency signature was proven to be effective in identifying and removing the low frequency component of the noise spectrum which overlapped the deep source signal spectrum.

5. A combination of non linear filtering followed by low pass linear filtering when applied to data recorded close to the ground level was found to optimise the signal to noise ratio when the signal was of deep origin and the noise was broad band from a near surface source.

6. The signal to noise ratio achievable after filtering was plotted against sensor elevation above a broad bandnoise source. From this curve it was concluded that the most cost effective survey for achieving near optimum signal resolution would be conducted at a noise source clearance of about two metres and a sample interval of two metres. The worst signal to noise ratio would be achieved from a low level (typically helicopter) airborne survey with a sensor at 10 metres above the noise source. (the signal to noise ratio was then reduced by a factor of fifteen). If the requirement of rapid large area coverage were to prescribe an airborne survey, then the optimum sensor elevation would be 75 metres in this situation. The compromise in using an airborne survey at the optimum elevation must be a factor of five reduction in signal to noise ratio.

7. In the case of Elura, the combination of nonlinear and low pass filtering produced data in which less than 2% of the profile energy was attributable to the maghemitic noise source.

8. The relative signal to noise ratio achievable at different sensor heights above a white noise source was used to predict to what depth a signal from a target of given size and magnetic susceptibility could be detected beneath a predicted intensity of noise. As a very conservative criterion for the detection of a signal, it was proposed that the signal to

noise ratio must exceed 5:1. Under ideal close-grid conditions where the anomaly has been traversed by several adjacent survey lines this ratio could be reduced to 1:1. In the case of the Elura orebody in the Elura noise environment, the signal to noise ratio for a ground level survey was predicted to exceed 5:1 had this body occurred at any depth down to 280 metres. Using the more optimistic 1:1 ratio criterion the Elura orebody would remain detectable to 475 metres.

The optimum elevation airborne survey at 75 metres would yield a signal to noise ratio greater than 5:1 for an Elura orebody source down to a depth of 155 metres. If the flight line spacing were 100 metres or less, then the body could have been detected down to a depth of 300 metres with a signal to noise ratio greater than 1:1.

In the worst case of a helicopter survey at 10 metres elevation Elura could only have been detected had it existed within 40 metres of the surface (5:1 ratio) or 165 metres (1:1 ratio).

9. A maghemitic palaeochannel near Cobar was considered as an example of an extremely severe noise source. In this case the intensity of the noise envelope was several thousand nT. It was concluded that had the Elura orebody existed beneath such a channel then it could have been detected from a ground level survey at any depth down to 25 metres (5:1 ratio) or 160 metres (1:1 ratio). The optimum elevation airborne survey at 75 metres could not detect the body at any depth with a signal to noise ratio greater than 5:1 and it could only detect it to a depth of 55 metres with a signal to noise ratio greater than 1:1. A survey flown at 10 metres elevation could not detect the body at all.

BIBLIOGRAPHY

Adams, R.L. and Schmidt, B.L. (1980). Geology of the Elura Zn-Pb-Ag deposit. The Proceedings of the Elura Symposium, Sydney. D.W. Emerson (ed.), *Bull. Aust. Soc. Explor. Geophys.*, 11(4): 143-146.

Anders, E.B., Johnson, J.J., Lasaine, A.D., Spikes, P.W. and Taylor, T.J. (1964). *Digital Filters.* NASA CR-136, O.T.S., Washington, Dept of Commerce, 132p.

Bacon, L.O. (1982). Personal communication.

Bacon, L.O. and Elliot, C.L. (1981). Redox chemical remanent magnetization - a new dimension in exploration for sulfide deposits in volcanic covered areas. *Geophysics*, 46(8): 1169-1181.

Baker, C.J. (1978). *Geology of the Cobar 1:100,000 Sheet.* Geological Survey of New South Wales, Department of Mines, 51p.

Baker, C.J., Schmidt, B.L. and Sherwin, L. (1975). Revised stratigraphy of the Cobar-Gunderbooka area. Q. Notes Geol. Surv. N.S.W., 20, 14p.

Bednar, J.B. (1983). Applications of median filtering to deconvolution, pulse estimation, and statistical editing of seismic data. *Geophysics*, 48: 1598-1610.

Bhattacharyya, B.K. (1966). Continuous spectrum of the total magnetic field anomaly due to a rectangular prismatic body. *Geophysics*, 31: 97-121.

Bhattacharyya, B.K. (1972). Design of spatial filters and their application to high-resolution aeromagnetic data. *Geophysics*, 37(1): 68-91.

Bhattacharyya, B.K. (1976). Recursion filters for digital processing of potential field data. *Geophysics*, 41: 712-726.

Bhattacharyya, B.K. (1980). A generalized multibody model for inversion of magnetic anomalies. *Geophysics*, 45(2): 255-270.

Blackburn, G. (1980). Gravity and Magnetic Survey-Elura orebody. *Bull. Aust. Soc. Explor. Geophys.*, 11(4): 17-24.

Blackman, R.B. and Tukey, J.W. (1958). *The Measurement of Power Spectra.* Dover Publications, Inc., New York, 181p.

Blair, D.P. and Spathis, A.T. (1980). Some aspects of digital filtering. Technical Report No. 118, Division of Applied Geomechanics, Institute of Earth Sciences, CSIRO, 30p.

Bracewell, R.M. (1978). *The Fourier Transform and Its Application.* McGraw Hill, New York, 433p.

Brooke, W.J.L. (1976). Cobar copper, lead, zinc deposits; in ore deposits of the Lachlan Fold Belt, New South Wales. 25th International Geological Congress, Excursion Guide, 15C, pp. 25-30.

Claerbout, J.F. and Muir, F. (1973). Robust modelling with erratic data. *Geophysics*, 38: 826-844.

Clark, D. (1980). Discussion Elura Symposium, Sydney. *Bull. Aust. Soc. Explor. Geophys.*, 11(4): 332.

Clark, P.J. (1981). Caesium vapour and proton precession magnetometer surveys in the Gipsies Range. Honours Thesis, The University of New England, 50p.

Clarke, G.K.C. (1969). Optimum second-derivative and downward continuation filters. *Geophysics*, 34: 424-437.

Darby, E.K. and Davies, E.B. (1967). The analysis and design of two-dimensional filters for two-dimensional data. *Geophys. Prosp.*, 15: 383-406.

Davis, L.W. (1980). The discovery of Elura and a brief summary of subsequent geophysical tests at the deposit. *Bull. Aust. Soc. Explor. Geophys.*, 11(14): 147-151.

Dean, W.C. (1958). Frequency analysis for gravity and magnetic interpretation. *Geophysics*, 23: 97-127.

Deer, W.A., Howie, R.A. and Zussman, J. (1964). *Rock-Forming Minerals.* Longman, Green and Co. Ltd, Vol. 5, 365p.

Emerson, D.W. (1980). The Elura compendium. The Proceedings of the Elura Symposium, Sydney. D.W. Emerson (ed.), *Bull. Aust. Soc. Explor. Geophys.*, 11(4).

Gallagher, N.C. and Muir, F. (1981). A theoretical analysis of median filters. *I.E.E.E., Trans. Acoustics, Speach & Signal processing*, 29: 1136-1141.

Gidley, P.R. and Stuart, D.C. (1980). Magnetic property studies and magnetic surveys of the Elura prospect, Cobar, N.S.W. The Proceedings of the Elura Symposium, Sydney. D.W. Emerson (ed.), *Bull. Aust. Soc. Explor. Geophys.*, 11(4): 167-172.

Gilligan, L.B. and Suppel, D.W. (1978). Mineral deposit in the Cobar supergroup and their structural setting. Q. Notes Geol. Surv. N.S.W., 33, pp. 15-22.

Grant, F.S. (1972). Review of data processing and interpretation methods in gravity and magnetics. *Geophysics*, 37: 647-661.

Grant, F.S. and West, G.F. (1965). *Interpretation Theory in Applied Geophysics*. International Series in the Earth Sciences, McGraw-Hill Book Company, 577p.

Green, A.G. (1972). Magnetic profile analysis. *Geophys. J.R. astr. Soc.*, 30: 393-403.

Gupta, V.K. and Ramani, N. (1980). Some aspects of regional-residual separation of gravity anomalies in a Precambrian terrain. *Geophysics*, 45(9): 1412-1426.

Hahn, A. (1965). Two applications of Fourier's analysis for the interpretation of geomagnetic anomalies. *J. geomag. Geoel.*, 17(3-4): 195-225.

Hahn, A., Kind, E.G. and Mishra, D.C. (1976). Depth estimation of magnetic sources by means of Fourier amplitude spectra. *Geophys. Prosp.*, 24: 287-308.

Hamming, R.W. (1977). *Digital Filters*. Prentice-Hall Signal Processing Series. Alan V. Oppenheim Series edition.

Henderson, R.G. (1960). A comprehensive system of automatic computation in magnetic and gravity interpretation. *Geophysics*, 25: 569-585.

Henderson, R.G. (1970). On the validity of the use of the upward continuation integral for total magnetic intensity data. *Geophysics*, 35(5): 916-919.

Henderson, R.G. and Zietz, I. (1949). The upward continuation of anomalies in total magnetic intensity fields. *Geophysics*, 14: 517-534.

Holloway, J.L. (1958). Smoothing and filtering of time series and space fields. *Advances in Geophysics*, Academic Press, Inc., 4: 351-391.

Jenkins, G.M. and Watts, D.G. (1968). *Spectral Analysis and Its Applications*. Holden-Day, Inc., San Francisco, 515p.

Kappelle, K. (1970). Geology of the C.S.A. mine, Cobar, N.S.W. Proceedings of the Australian Institute of Mining Metallurgy, 233: 79-94.

Le Borgre, E. (1960). The influence of fire on the magnetic properties of soil, schist and granite. *Annals Geophysics*, 16: 159-196.

Lehmann, H.J. (1970). Examples for the separation of fields of magnetic sources in different depths by the harmonic analysis method. *Boll. Geofis. Teor. Appl.*, 12: 97-117.

Lynn, P.A. (1980). *An Introduction to the Analysis and Processing of Signals.* The Macmillan Press Ltd., 221p.

Naidu, P.S. (1967). Two-dimensional Strakhov's filter for extraction of a potential field signal. *Geophys. Pros.,* 15: 135-150.

Oppenheim, A.V. and Schafer, R.W. (1975). *Digital Signal Processing.* Prentice-Hall,Englewood Cliffs, New Jersey, 585p.

Ota, Kulhanek (1976). *Introduction to the Digital Filtering in Geophysics.* Elsevier Scientific Publishing Company, Amsterdam-Oxford-New York, 195p.

Otnes, R.K. and Enochson, L. (1972). *Digital Time Series Analysis.* A Wiley-Interscience Publication, John Wiley & Sons, 461p.

Peters, L.J. (1949). The direct approach to magnetic interpretation and its practical application. *Geophysics,* 14: 290-320.

Pogson, D.J. and Felton, E.A. (1978). Reappraisal of geology, Cobar-Canbelego-Mineral Hill region, central western N.S.W. Q. Notes Geol. Surv. N.S.W., 33, pp. 1-14.

Pogson, D.J., Suppel, D.W., Gilligan, L.B., Scheibner, E., Baker, C., Sherwin, L., Brown, R., Felton, E.A. and Fail, A.P. (1976). Recent studies of the tectonics, stratigraphy and mineralization of the Cobar-Mineral Hill region. *Bull. Aust. Soc. Explor. Geophys.,* 7(1): 31-34.

Robinson, E.A. and Treitel, S. (1967). Principles of digital wiener filtering. *Geophysics,* 15(3): 395-404.

Robinson, E.S. (1970). Upward continuation of total intensity magnetic fields. *Geophysics,* 35(5): 920-926.

Sangster, D.F. (1979). Evidence of an exhalative origin for deposits of the Cobar district, New South Wales. *BMR J. Aust. Geol. Geophys.,* 4: 15-24.

Scheibner, E. and Markham, N.L. Tectonic setting of some strata-bound massive sulphide deposits in New South Wales, Australia. K.H. Wolf (ed.), *Handbook of Strata-bound and Stratiform Ore Deposits,* Vol. 6, Elsevier Scientific Publishing Company, 583p.

Shanks, J.L. (1967). Recursive filters for digital processing. *Geophysics,* 32(1): 33-51.

Shanks, J.L. (1969). Two-dimensional recursive filters. *SWIEEECO Rec.,* pp. 19E1-19E8.

Shanks, J.L., Treitel, S. and Justice, J.H. (1972). Stability and synthesis of two-dimensional recursive filters. *IEEE Trans. Audio Electro-acoust.,* AU-20: 115-128.

Sheriff, R.E. (1980). *Encyclopedic Dictionary of Exploration Geophysics.* Society of Exploration Geophysicists, Tulsa, Oklahoma, 265p.

Skrzeczynski, R.H. and Meates, G.R. (1977). Final report on exploration Cobar joint venture, Cobar, N.S.W. Utah Development Company Exploration Department, Report No. 292, unpublished.

Spector, A. and Grant, F.S. (1970). Statistical models for interpreting aeromagnetic data. *Geophysics,* 35: 293-302.

Spies, B.R. (1978). A combined ground geophysical survey in an area of poor outcrop west of the S. Alligator river, N.T. (used TEM, EM (gun), VLF, magnetic and resistivity). BMR Report No. 205 (BMR Microfiche 29).

Stacey, F.D. and Banerjee, S.K. (1974). *The Physical Principles of Rock Magnetism.* Elsevier, Amsterdam, pp. 92-95.

Stanley, J.M. (1975a). An lakali vapour magnetometer and its applications. Ph.D. Thesis, The University of New England, Armidale, Australia.

Stanley, J.M. (1975b). Application of a rapid sampling vehicle-borne magnetometer. *Bull. Aust. Soc. Explor. Geophys.,* 6(4): 100-103.

Stanley, J.M. (1979). The discussion of Wilkes' paper at the Applied Magnetic Symposium in Sydney. *Bull Aust. Soc. Explor. Geophys.,* 10(1): 113-114.

Stanley, J.M. (1982). New magnetometer technology and its application to archaeological exploration. W. Ambrose and P. Duerden (eds), *Archaeometry: An Australasian Perspective,* pp. 151-155.

Strakhov, V.N. (1964). The smoothing of observed strengths of potential fields, I. *Izv. Geophysics,* Series No. 10, pp. 1479-1493.

Strakhov, V.N. and Lapina, M.I. (1967). A method of smoothing potential fields. *Akad. Nank. SSSR Izv. Ser. Fixika Zemli,* pp. 40-57.

Tite, M.S. and Linington, R.E. (1975). Effect of climate on the magnetic susceptibility of soils. *Nature,* 256: 565-566.

Tsay, L.J. (1978). A spatial analysis of upward continuation of potential field data. *Geophys. Prosp.,* 26: 822-840.

Wainstein, L.A. and Zubakov, V.D. (1962). *Extraction of Signals from Noise* (translated from Russian). Prentice-Hall, Englewood Cliffs, New Jersey, 349p.

Wiener, N. (1949). *Extrapolation, Interpolation and Smoothing of Stationary Time Series.* J. Wiley & Sons, New York, 280p.

Wilkes, P.G. (1979). Characteristics of magnetic sources and guidelines for exploration in the Cobar area, N.S.W. *Bull. Aust. Soc. Explor. Geophys.*, 10(1): 34-41.

Zurflueh, E.G. (1967). Application of two-dimensional linear wavelength filtering. *Geophysics*, 32: 1015-1035.

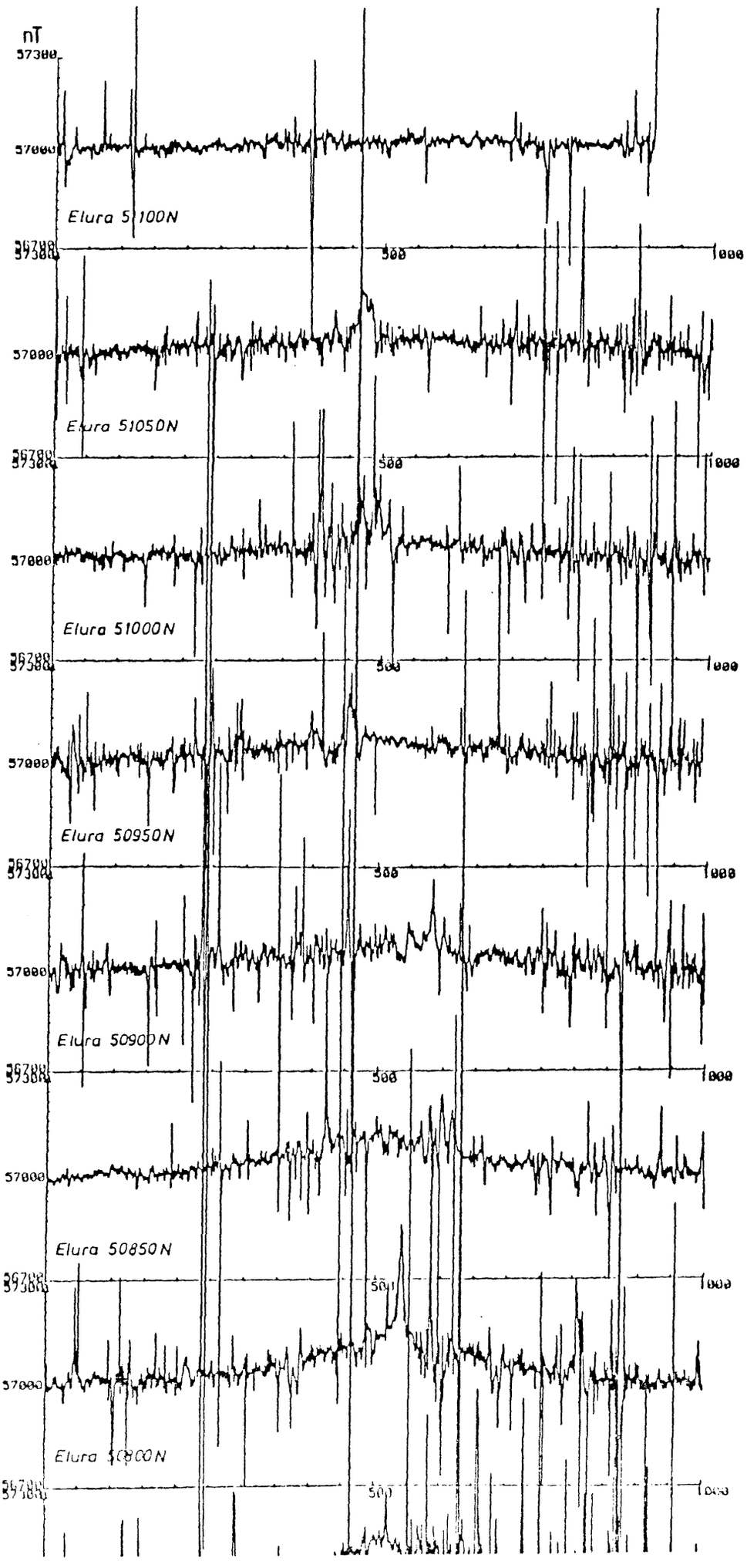
nT
57300
57000
Elura 51100N
500
1000
Elura 51050N
Elura 51000N
Elura 50950N
Elura 50900N
Elura 50850N
Elura 50800N

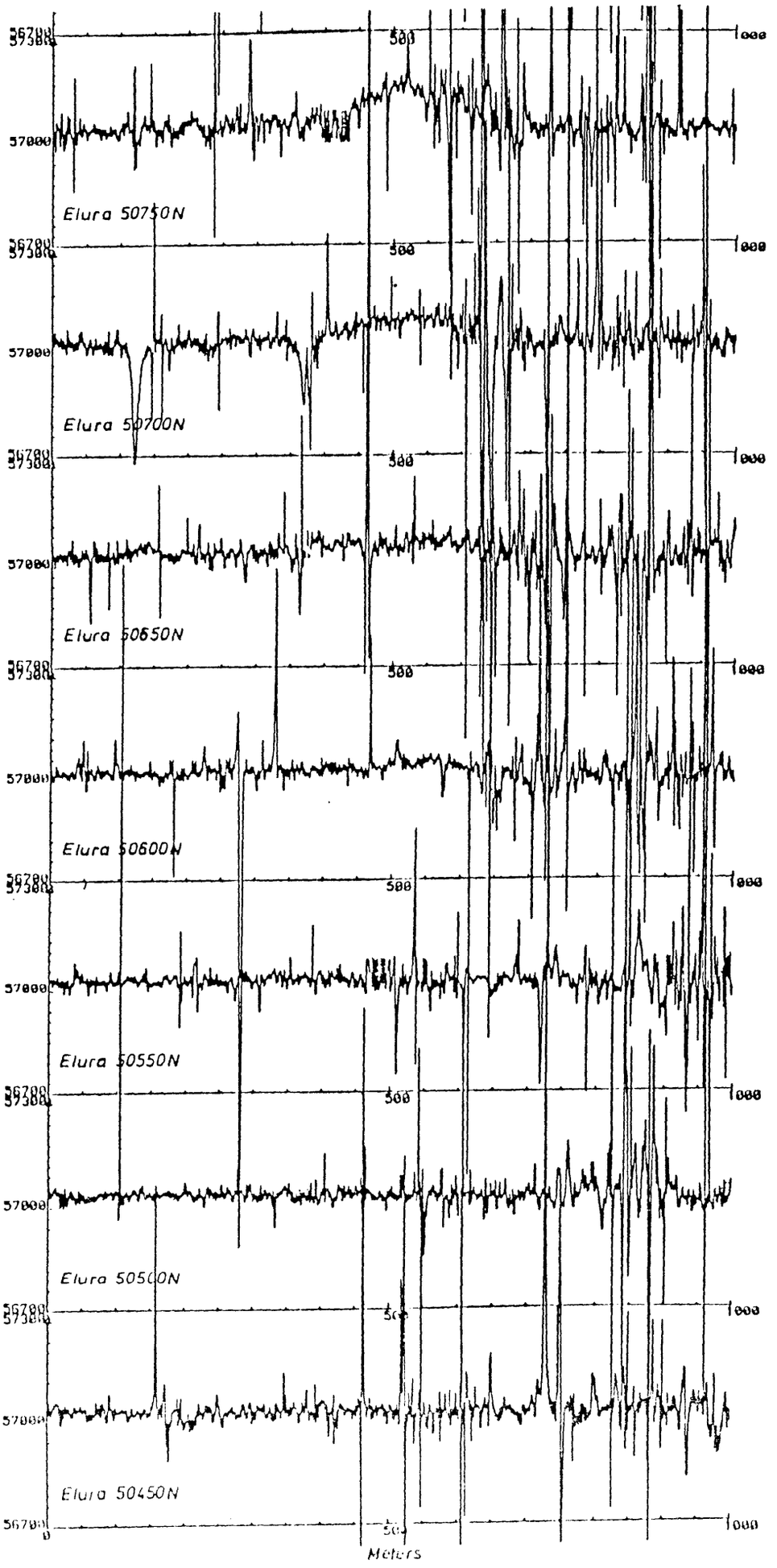
Elura 50750N
Elura 50700N
Elura 50650N
Elura 50600N
Elura 50550N
Elura 50500N
Elura 50450N
Meters

APPENDIX II

Program FFT

```
C-------------------------------------------------------------------C
C This program is for spectrum calculation with subroutine        C
C FFT. Input data are in one column, for example                   C
C    57000.0                                                      C
C    56700.0                                                      C
C    57800.0   etc.                                               C
C                                                                 C
C  compiled by P. Clark.                                          C
C Semori Sertsrivanit,geophysics ONE,Armidale.                    C
C-------------------------------------------------------------------C

      Dimension x(8200),amp(8200)
      Complex cx(8200)
      Dimension Buffer(4)
C
1     Write(5,10)
10    Format(' enter the input file:'$)
      Read(5,15) Buffer
15    Format(4a5)
      Open(unit=20,access='seqin',dialog=buffer,err=1)
      i = 1
29    read(20,30,end=99) x(i)
c30    format(//,(10F7.1))
30    format(g)
      i = i+1
      go to 29
99    n = i-1
      write(5,16)n
16    format(' Number data points:',I6)
C
      write(5,161)
161   format(' Data sample interval = '$)
      read(5,162) dt
162   format(g)
C-------------------------------------------------------------------C
C  Remove trend and end effect                                      C
C-------------------------------------------------------------------C
      call trend(x,n,dcx,slope)
      Write(5,90) dcx,slope
90    Format(' Dc level of Time series =',g,/
     1       ' Slope =',g)
      call taper(x,n)
```

```
C-----------------------------------------------------------------C
C  Complexcity                                                    C
C-----------------------------------------------------------------C
      do  44   i=1,n
      cx(i) = cmplx(x(i),0.0)
44    continue
      Write(5,91)
91    format(' number power nu = "$)
      read(5,92) nu
92    format(I2)
C-----------------------------------------------------------------C
C Transform data by Fast Fourier Transform and compute the       C
C Energy spectrum                                                C
C-----------------------------------------------------------------C
      call nlogn(nu,cx,-1.0,n)
C
      n2 = n/2+1
      dn = 2.0*dt/float(n)
      do  55  i=1,n2
      amp(i) = dn*(real(cx(i))**2+aimag(cx(i))**2)
55    continue
C-----------------------------------------------------------------C
C  Sum of the energy spectrum from zero to nyquist frequency     C
C-----------------------------------------------------------------C
      sum = 0.0
      do  106  i=1,n2
      sum = sum+amp(i)
106   continue
      type 717, sum
717   format(' sum = ',g)
C-----------------------------------------------------------------C
C  Write output of the energy spectrum                            C
C-----------------------------------------------------------------C
2     Write(5,56)
56    Format(' Output file name:'$)
      Read(5,15) buffer
      Open(unit=21,access='seqout',dialog=buffer,err=2)
      do  221   i=1,n2
221   write(21,77) amp(i)
77    format(g)
C
      stop
      end
C
```

```
      Subroutine nlogn(n,x,sign,lx)

C-----------------------------------------------------------------C
C lx-the number of points in array x                              C
C nmax-the largest value of nu to be processed                    C
C nondummy dimension m(nmax)                                      C
C dimension x(2**n)                                               C
C For example,if nmax=25 then                                     C
C-----------------------------------------------------------------C

      Dimension m(25)
      Dimension x(lx)
      Complex x,wk,hold,q
      pi = 3.1415926
      Do  1   i=1,n
1     m(i) = 2**(n-i)
      Do  4   L=1,n
      nblock = 2**(L-1)
      Lblock = Lx/nblock
      Lbhalf = Lblock/2
      k = 0
      Do  4   iblock=1,nblock
      fk = k
      flx = Lx
      v = sign*2.0*pi*fk/flx
      wk = cmplx(cos(v),sin(v))
      istart = Lblock*(iblock-1)
      Do  2   i=1,lbhalf
      j = istart+i
      jh = j+Lbhalf
      q = x(jh)*wk
      x(jh) = x(j)-q
      x(j) = x(j)+q
2     continue
      Do  3   i=2,n
      ii = i
      if(k .lt. m(i)) go to 4
3     k = k-m(i)
4     k = k+m(ii)
      k = 0
      Do  7   j=1,Lx
      if(k .lt. j) go to 5
      hold = x(j)
      x(j) = x(k+1)
      x(k+1) = hold
5     Do  6   i=1,n
      ii = i
      if(k .lt. m(i)) go to 7
6     k = k-m(i)
7     k = k+m(ii)
      if(sign .lt. 0.0) return
```

```
      Do  8   i=1,Lx
8     x(i) = x(i)/flx
      return
      End
C-----------------------------------------------------------------C
      Subroutine Trend(array,n,dclev,slope)
      Dimension array(n)
       Sum = 0.0
       Do  1   i=1,n
1      Sum = sum+array(i)
       dclev = sum/float(n)
       slope = 0.0
       nu = n/3
       k = n-nu
       Do  3   i=1,nu
       j = k+i
3      slope = slope+array(j)-array(i)
       slope = slope/float(nu*k)
       r = -float(n+1)*0.5
       Do  4   i=1,n
4      array(i) = array(i)-dclev-slope*(float(i)+r)
       return
       End
C-----------------------------------------------------------------C
      Subroutine Taper(x,L)
      Dimension x(L)
       pi = 3.1415926
       nt = L/10
       PI = pi/float(nt)
C-----------------------------------------------------------------C
C  applies a taper to each 10% end of data                        C
C  last point set to 0.0                                          C
C  this should gives good cyclic match for stationary process     C
C-----------------------------------------------------------------C
       Do  1   i=1,nt
       k = L-i
       Tap = 0.5*(1.0-cos(PI*float(i)))
       x(i) = x(i)*tap
1      x(k) = x(k)*tap
       x(L) = 0.0
       return
       End
```

APPENDIX III

Program Filter

```
C-------------------------------------------------------------C
C   This program is a standard Butterworth filter.            C
C   Dimension(x and y) should be double of number data points  C
C   Input data are in one column,example                       C
C      57000.60                                                C
C      57090.10                                                C
C      57050.00  etc.                                          C
C                                                              C
C   zero level can be either mean(Or average value which will  C
C   be computed by the computer and seen in the screen after   C
C  running the program) or base field value.                   C
C  modified from a program by P. Clark.                        C
C Somsri Sertsrivanit,geopgysics UNE,Armidale.                 C
C-------------------------------------------------------------C

      Dimension x(26400),y(26400)
      Dimension Buffer(4)
      Dimension c(3),a0(3),a1(3),a2(3),b1(3),b2(3)
C
1     Write(5,10)
10    Format('0Enter the input file:'$)
      Read(5,15) Buffer
15    Format(4a5)
      Open(unit=20,access='seqin',dialog=buffer,err=1)
      i = 1
99    Read(20,30,end=999) x(i)
30    format(g)
      i = i+1
      go to 99
999   nt = i-1
C
      Write(5,81)nt
81    Format(' Number data points = ',I6)
C
      sum = 0.0
      do  290   i=1,nt
290   sum = sum+x(i)
      av = sum/float(nt)
      type 34,av
34    format(' Average value =',F)
      write(5,409)
409   format(' What is the zero level? :'$)
      read(5,208) ixav
208   format(I6)
      xav = float(ixav)
```

```
      Do  291   i=1,nt
      y(i) = x(i)-xav
291   continue
      do  219  j=1,nt
      x(j) = y(j)
219   continue
C-----------------------------------------------------------------C
C     This routine applies the 6th order Butterworth filter      C
C     And pass the filter twice to have a zero phase             C
C     Adding ndt points of exponential taper to front and        C
C     rear of time waveform.This minimizes end effects           C
C     due to filtering.                                          C
C-----------------------------------------------------------------C
      ndt = nt/8
      nt = nt+ndt
      nn = nt-ndt
      do  401   j=1,nn
401   x(nt-j+1) = x(nn-j+1)
      g = float(ndt)
C-----------------------------------------------------------------C
C     Waveform tapers to exp(-5) using ffa                       C
C-----------------------------------------------------------------C
      ffa = float(ndt)/5.0
      Do  402   j=1,ndt
      F = float(j)
      fac = (F-g)/ffa
402   x(j) = x(ndt+1)*exp(+fac)
      Do  403   j=1,ndt
      F = float(ndt-j+1)
      fac = (F-g)/ffa
403   x(nt+j) = x(nt)*exp(fac)
      nt = nt+ndt
      Write(5,41)
41    Format(' Cut-off frequency in cycles/meter?:'$)
      Read(5,106) Fc
      PI = 3.1415926
      Wc = 2.0*PI*Fc
      Write(5,107)
107   Format(' Sampling interval(DT) in meter?:'$)
      Read(5,106) DT
106   Format(g)
      T = Wc*DT
      C(1) = 0.5176
      C(2) = 1.4142
      C(3) = 1.9318
      Do  11   J=1,3
      FAC = T*T+2.0*C(J)*T+4.0
      A0(J) = T*T/FAC
      A1(J) = 2.0*A0(J)
      A2(J) = A0(J)
      B1(J) = (2.0*T*T-8.0)/FAC
11    B2(J) = (T*T-2.0*C(J)*T+4.0)/FAC
```

```
      NPASS = 0
      K = 1
22    Y(1) = A0(K)*X(1)
      Y(2) = A0(K)*X(2)+A1(K)*X(1)-B1(K)*Y(1)
      Do  18  J=3,nt
      Y(J) = A0(K)*X(J)+A1(K)*X(J-1)+A2(K)*X(J-2)
18    Y(J) = Y(J)-B1(K)*Y(J-1)-B2(K)*Y(J-2)
      Do  13   J=1,nt
13    X(J) = Y(J)
      K = K+1
      If(K .le. 3) go to 22
      If(npass .eq. 1) go to 54
C-----------------------------------------------------------------C
C     Reverse output to pass the 2nd pass filter                  C
C-----------------------------------------------------------------C
      Do  26   j=1,nt
26    X(J) = Y(nt-J+1)
      Npass = 1
      K = 1
      go to 22
54    continue
C-----------------------------------------------------------------C
C     Reverse time output                                         C
C-----------------------------------------------------------------C
      Do  27   j=1,nt
      x(j) = y(nt-j+1)
27    continue
C-----------------------------------------------------------------C
C     Subtracting ndt points from front and rear of waveform      C
C     to leave original length of data                            C
C     Data points x(1) up to x(nt) comprise original data         C
C     length But filtered                                         C
C     Obtain output from 2nd recursive butterworth filter       - C
C-----------------------------------------------------------------C
2     Write(5,110)
110   Format('0Out put file name:'$)
      Read(5,15) Buffer
      Open(unit=21,access='seqout',dialog=Buffer,err=2)
      m = ndt+1
      mm = nt-ndt
      Do  405   i=m,mm
      y(i) = x(i)
      write(21,33) y(i)
33    format(g)
405   continue
C
      Stop
      End
```

APPENDIX IV

Program despike .

```
C-------------------------------------------------------------------C
C   This program reads data which is in one column for a          C
C   process of despiking.                                         C
C   Example of the data format is:                                C
C      57000.0                                                    C
C      57600.0                                                    C
C      57500.0  etc.                                              C
C                                                                 C
C   modified by P. Clark from a program by R. Green.              C
C   Somsri Sertsrivanit,geophysics UNE,Armidale.                  C
C-------------------------------------------------------------------C

      Real  x(13000),y(13000)
      Dimension buffer(4)
C
1     write(5,10)
10    format('0Input name:'$)
      read(5,15) buffer
15    format(4a5)
      open(unit=20,access='seqin',dialog=buffer,err=1)
      i = 0
115   read(20,19,end=99) x(i)
19    format(g)
      i = i+1
      go to 115
99    n = i-1
C
      write(5,16) n
16    format(' Number data points =',I6)
C-------------------------------------------------------------------C
C  Input 'WINDOW' and 'RANGE'                                       C
C-------------------------------------------------------------------C
      write(5,61)
61    format(' Window(number points) = '$)
      read(5,62) iwn
62    format(I5)
      write(5,63)
63    format(' What is the RANGE(nT)? ='$)
      read(5,62) irang
      range = float(irang)
      npass = 0
24    do  55  j=iwn,n
      sum = 0.0
```

```
        do  56  i=j-(iwn-1),j
        sum = sum+x(i)
56      continue
        av = sum/float(iwn)
        tk = av+range
        tr = av-range
        if(x(j+1) .gt. tk) x(j+1)=av
        if(x(j+1) .lt. tr) x(j+1)=av
        y(j-iwn+1) =av
55      continue
        if(npass .eq. 1) go to 54
C-------------------------------------------------------------C
C  Reverse output data to pass the 2nd pass despike           C
C-------------------------------------------------------------C
        do  27  j=1,n
        y(j) = x(n-j+1)
27      continue
        do  28  i=1,n
        x(i) = y(i)
28      continue
        npass = 1
        go to 24
54      continue
C-------------------------------------------------------------C
C  Reverse the 2nd pass despiked data to obtain the output    C
C-------------------------------------------------------------C
        do  29   k=1,n
        y(k) = x(n-k+1)
29      continue
C
2       write(5,35)
35      format('0Output name:'$)
        read(5,15) buffer
        open(unit=22,access='seqout',dialog=buffer,err=2)
        write(22,45) (y(j), j=1,n)
45      format(g)
        stop
        end
```